University of Stavanger

Faculty of Science and Technology

MASTER'S THESIS

Study program/ Specialization: MSc Petroleum Engineering / Reservoir Engineering	Spring semester, 2016 Open access
Writer: Anggi Putra Yanse	…… (Writer's signature)
Faculty supervisor: Professor II, Leif Larsen External supervisor(s): Senior Research Engineer, Anton Shchipanov	
Thesis title: Designing Well Tests to Understand Performance of Induced Fractures	
Credits (ECTS): 30	
Key words: Induced Fracture Fracture Orientation Numerical Simulations Analytical Well Testing Interference Tests Single-Well Tests	Pages : 51 + enclosure : 13 Stavanger, 15 june 2016

Designing Well Tests to Understand Performance of Induced Fractures

Master Thesis

By

Anggi Putra Yanse

Supervisor:

Senior Research Engineer
Anton Shchipanov

Supervisor:

Professor II
Leif Larsen

International Research Institute
Stavanger

Faculty of Engineering and Science
University of Stavanger

Summary

Presently, more and more water injection wells operate under induced fracturing condition. Induced fractures geometry and their orientation with respect to the injection well and nearby production wells are crucial factors in determining water injection performance. Designing, conducting and interpreting well tests is a possible way to understand geometry and dynamic behavior of induced fractures. Integrating nearby wells into well testing may give a possibility to characterize induced fracture geometry and its impact on macroscopic sweep efficiency.

In this thesis, one of the objectives is getting knowledge on pressure transient responses of wells connected with fractures with different geometries and orientations using numerical simulations and analytical models. Two scenarios of well tests including single-well tests and interference tests were simulated with two well geometries (vertical and horizontal) and two induced fracture orientations (parallel and perpendicular to the well). Base cases without fracture were simulated and compared with cases including induced fractures. The numerical simulation included injection periods and shut-in periods with similar durations. Synthetic responses generated by the numerical simulation were compared with well test responses from equivalent analytical models. Comparison between the results of all fracture cases for single-well tests and also interference tests were performed and subsequently used to analyse differences in pressure transient responses. Moreover, a comparison of the results of numerical simulations with analytical models was carried out and confirmed capabilities of analytical models in interpreting pressure responses from many cases with various well and fracture geometries.

The analysis of single-well test simulations confirmed that the case with parallel and perpendicular induced fractures intersecting a horizontal well has identical pressure transient responses to the case of induced fracture intersecting a vertical well for cases with high or infinite conductivity. On the other hand, interpretations of the synthetic pressure response generated by simulations of well interference tests indicated different responses in the case with parallel and perpendicular induced fractures: the pressure response to the active well shut-in (or start of injection) was registered later in the observation well in the case of parallel fracture. Therefore, it was confirmed that interference tests can give more information about fracture orientation than single-well tests. Finally, it was shown the value of interpretations of synthetic pressure transients in understanding induced fracture geometry and suggesting a well test design for the field application.

Acknowledgements

Thanks God Almighty for the wisdom and perseverance that He has been bestowed upon me during this thesis, and indeed, throughout my life.

It is a great pleasure to acknowledge my deepest thanks and gratitude to Senior Research Engineer Anton Shchipanov, my supervisor at IRIS for suggesting the topic of my thesis. His guidance, advices, and support throughout the thesis project are greatly appreciated.

I would like to thank my supervisor at University of Stavanger, Professor Leif Larsen for his advices and detailed review during the thesis work.

My thanks also go out to my parents in Indonesia for their love, prayers, and blessings during my study abroad.

And finally, thanks to all my friends during my study in Stavanger who were always help and encourage me in numerous ways.

Table of Contents

SUMMARY ..... **I**

ACKNOWLEDGEMENTS ..... **II**

TABLE OF CONTENTS ..... **III**

LIST OF FIGURES ..... **V**

LIST OF TABLES ..... **VII**

1. INTRODUCTION **1**

1.1. OBJECTIVE 1
1.2. SCOPE OF WORK 1

2. THEORETICAL BACKGROUND **3**

2.1. THEORY OF PRESSURE TRANSIENT ANALYSIS AND WELL TESTING 3
2.1.1. Types of Pressure Transient Test 3
2.1.2. Drawdown and Build up Tests 4
2.1.3. Injection and Fall-off Tests 4
2.1.4. Pressure Derivatives 4
2.1.5. Flow Regimes in Pressure Transient Test 5
2.1.6. Interference Test 5
2.2. HYDRAULIC FRACTURING 6
2.2.1. Fracture Orientation 6
2.2.2. Fractured wells in well testing 8
2.2.3. Fractured Horizontal Well 9
2.2.4. Determination of Fracture Orientation 10
2.2.5. Induced Fracture in Injection Well 11
2.3. PRESSURE (STRESS) DEPENDENT PERMEABILITY 12

3. NUMERICAL SIMULATION AND ANALYTICAL WELL TESTS **13**

3.1. SIMULATION MODEL DESCRIPTION 14
3.2. EFFECT OF GRID SIZE IN NUMERICAL SIMULATIONS 15
3.3. FRACTURE GRID BLOCK 15
3.4. NUMERICAL SIMULATION OF WELL TEST SCENARIOS 16
3.4.1. Single Well-Test Scenarios 16
3.4.2. Interference Test Scenarios 20
3.5. ANALYTICAL WELL TEST SCENARIOS 24

4. RESULTS AND DISCUSSION **26**

4.1. SINGLE-WELL TESTS 26
4.1.1. Comparison between Analytical and Numerical simulations in Non Fractured Well 26

4.1.2. Effect of Fracture Conductivity on PTA Responses 28
4.1.3. Effect of Induced Fracture Direction in Vertical and Horizontal Wells ... 28
4.1.4. Impact of Fracture Distance in Multiple Transverse Fracture Case 32
4.1.5. Conclusion of Single-Well Tests Study 33
4.2. INTERFERENCE TESTS 33
4.2.1. Comparison between Numerical and Analytical Simulations in Interference Tests (Non Fractured Well Cases) 33
4.2.2. Comparison between Longitudinal Induced Fracture and Transverse Induced Fracture in Interference Test 35
4.2.3. Impact of Pressure Dependent Fracture Permeability 38
4.2.4. Comparison to Analytical Well Tests Study 40
4.2.5. Conclusions of Interference Test Study 41
5. CONCLUSIONS 43
REFERENCES 45
NOMENCLATURE 49
ABBREVIATIONS 51
APPENDIX 52

List of Figures

Figure 1: Model for pressure transient analysis and well test interpretation (adapted from Horne, 1995) 3
Figure 2: Log-log scales of Theis solutions. Pressure and derivative responses. (adapted from Bourdet, 2002) 6
Figure 3: Fracture orientation in the vertical well 7
Figure 4: Fracture orientation in the horizontal well (adapted from E.Fjaer et al. 2008) 7
Figure 5: Flow regime in fractured wells (adapted from Cinco-Ley and Samaniego, 1981) 8
Figure 6: The comparison of pressure and derivative between uniform flux and infinite conductivity fractures. (adapted from Cinco-Ley and Samaniego, 1981) 9
Figure 7: Type of flow regime in the horizontal well intercepted by fractures (adapted from Chen and Raghavan, 1997) 10
Figure 8: Impact of induced fracture direction on areal sweep (adapted from Husted et al. 2006) 11
Figure 9: Illustration of FAST technique. Fracture induced in the injector well because of injection pressure (adapted from Rod et al. 2005). 12
Figure 10: Workflow for combining numerical and analytical PTA 13
Figure 11: A reservoir model in numerical simulation 14
Figure 12: Synthetic pressures and derivatives for vertical well injector. Sensitivity on the grid size 15
Figure 13: Gradual LGR in fracture grid block 16
Figure 14: Injection well location 17
Figure 15: Model illustration of induced fracture direction parallel (blue) and perpendicular (green) with Y coordinate 18
Figure 16: Fractured horizontal wells in numerical simulations 19
Figure 17: Illustration of multi transverse induced fractures 20
Figure 18: Model illustration for interference test of non-fractured vertical and horizontal injection wells in numerical simulation 21
Figure 19: Model illustration for interference test of fractured horizontal wells in numerical simulation 22
Figure 20: Simulated bottom-hole pressure (non fractured horizontal well case) 22
Figure 21: kfp plot 23
Figure 22: Reservoir and well initialization in PTA tool (Saphir) 24
Figure 23: Well and reservoir parameters in analytical PTA 25
Figure 24: Reservoir and well parameters in saphir interference tests 25
Figure 25: Comparison of analytical (line) and numerical (marker) simulations for base case 26
Figure 26: Analytical (dots) and numerical (line) responses, rate and pressure for base case 27
Figure 27: Pressures and derivatives for case 1. Injection and fall-off phases 27

Figure 28: Figure 4.4: Impact of fracture conductivity in the fractured vertical well. Pressures (dashed line) and derivatives (line with marker) 28
Figure 29: Pressures and derivatives for case 2 and case 3. Injection and fall-off phases 29
Figure 30: Pressures and derivatives for case 2 and 4. Injection and fall-off phases ... 29
Figure 31: Illustration of well elements in a well with infinite conductivity fracture .. 30
Figure 32: Pressures for case 4, 5 and 6. Injection and fall-off phases 31
Figure 33: Pressure derivatives for case 4, 5 and 6. Injection and fall-off phases 31
Figure 34: Effect of fracture distance in multiple transverse induced fractures. Injection and fall-off phases 32
Figure 35: Pressure profiles in an observation well for vertical and horizontal injection wells. 34
Figure 36: Pressures and derivatives of an observation well for vertical and horizontal injection (active) wells 35
Figure 37: Pressures and derivatives in an observation well for fractured horizontal well cases 36
Figure 38: Impact of fracture orientation on the pressure distribution (at 200 hour) ... 37
Figure 39: Impact of paralel fracture on the pressure distribution around an injection well (at 9 hour) 37
Figure 40: Pressure in an observation well for all induced fracture cases 38
Figure 41: Pressure derivatives in an observation well for all induced fracture cases . 39
Figure 42: Impact of fracture orientation and $kf(p)$ on the pressure distribution (at 200 hour) 39
Figure 43: Illustration for fractured active-observation wells (adapted from Meehan et al. 1989) 40
Figure 44: The pressure and derivative in the observation well for r_D = 2 (adapted from Meehan et al. 1989) 41

List of Tables

Table 1: Reservoir and fluid properties 14
Table 2: Induced fracture properties. Case 2 and case 3 18
Table 3: Induced fracture properties. Case 4, case 5 and case 6 19
Table 4: Observation well parameters 20
Table 5: Pressure dependent fracture permeability for a longitudinal fracture case (ROCKTAB) 23
Table 6: Pressure dependent fracture permeability for a transverse fracture case (ROCKTAB) 24

1. Introduction

Nowadays, hydraulic fracturing is widely used around the world to improve well performance and enhance sweep efficiency. Hydraulic fracturing of horizontal wells is preferable in offshore field operations providing improved sweep efficiency in well drainage areas.

In pressure maintenance and water-flooding projects, fractures may be induced around the injection well, thus increasing well injectivity. Geometry of induced fractures and their position with respect to the stimulated well and nearby wells are critical factors governing sweep efficiency of oil displacement.

A horizontal injection well intercepted by perpendicular induced fractures toward nearby production wells could provide good pathways for water flow and faster water breakthrough in the production wells. From the other side, parallel induced fractures intersecting the horizontal injector would provide favorable conditions for better areal sweep efficiency (Rod et al. 2005 and Husted et al. 2006). For those reasons, knowledge about induced fracture geometry and orientation becomes particularly important to sustain water-flooding strategies, i.e. positioning of the injector and producer (Wei et al. 1998).

As of today the simulation of well tests is particularly interesting to be used for understanding and characterizing fractured reservoirs (Morton et al. 2012, Pan et al. 2013, Shchipanov et al. 2014, Egya et al. 2016). The synthetic pressure transient generated by the simulation of fractured reservoirs is further used to interpret and analyze which features of fractures can be detected from well tests.

This thesis therefore presents numerical simulation cases where different geometries and positions of induced fractures and their impact of pressure transient responses are studied. This helps to give better understanding of geometry and behavior of induced fractures.

1.1. Objective

The main objective of this thesis is to study the effect of induced fracture orientation with respect to the stimulated well using Pressure Transient Analysis (PTA). We should achieve this goal by designing well tests with various induced fracture geometries using numerical and analytical simulations and interpretations of pressure transient responses. Simulated well tests without induced fractures are included as base cases for comparison with cases including induced fractures.

1.2. Scope of Work

The scope of work can be divided into the following tasks:

- Assembling a mechanistic (synthetic) segment reservoir model (3D) with and without induced fractures in Eclipse reservoir simulator.
- Simulation of well tests consisting of flowing and shut-in periods, i.e. bottom-hole pressure transients at specified rates.
- Simulation of induced fractures with different geometries and positions connected to vertical and horizontal injection wells.
- Analysis of the induced fracture geometry effects on simulated pressure transient responses.
- Setting up analytical models with constant fracture parameters and reservoir permeability in the Saphir PTA tool to match uploaded results from equivalent Eclipse simulations (to get the numerical simulations in line with the analytical models).
- Integrating an observation well into well test simulations. Analysis of possible ways of improving the understanding of induced fracture orientation by integrating both tested and observation wells into the test procedure (well interference test).
- Analysis of impact of introducing pressure dependent fracture conductivity on simulation results and the interpretation of pressure transients.

2. Theoretical Background

2.1. Theory of Pressure Transient Analysis and Well Testing

Pressure transient analysis is investigation of the pressure response as a function of time due to changes in the flow rate. The aim of Pressure Transient Analysis (PTA) is to acquire the parameters of well and formation such as skin effect, permeability, porosity, distance to boundary, fracture properties, initial and average reservoir pressure under dynamic conditions. PTA was commonly used in the petroleum industry to improve reservoir characterization and to complement the estimation of hydrocarbon in place with long-duration well tests before reservoir simulation became the major tool.

In pressure transient analysis, the pressure response is an output and the flow rate is an input (Horne, 1995). Meanwhile, in well test analysis, mathematical models are used to associate pressure transients as an output and flow rate history as an input (Horne, 1995). By matching pressure responses from field data to model outcomes we can conclude that the model properties have same value with reservoir properties.

Bourdet (2002) explained that pressure responses can be generated by numerical simulations or analytical solutions to the particular production or injection rate history of well, and the model parameters are adjusted until the model behavior is equal to the well and reservoir behavior.

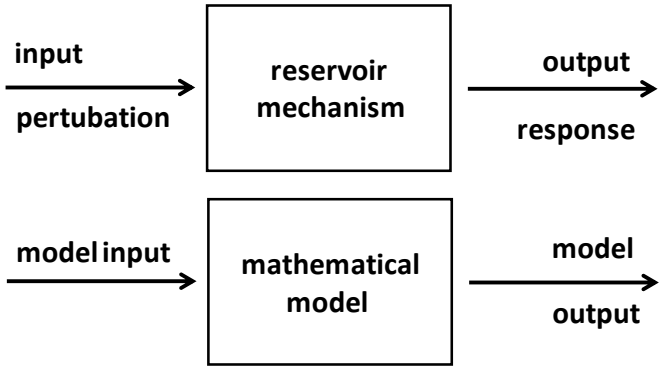

Figure 1: Model for pressure transient analysis and well test interpretation (adapted from Horne, 1995)

Nowadays, many companies use downhole gauges to measure the pressure change over time in order to monitor the well performance.

2.1.1. Types of Pressure Transient Test

There are various types of pressure transient tests. The choice of tests is based on the test purpose, type of wells and technical limitation.

2.1.2. Drawdown and Build up Tests

In drawdown tests, the well is flowing with a constant rate. In general, the well is shut in first before conducting the drawdown tests to achieve downhole pressure equal to static reservoir pressure. This test has an economic benefit for the company due to the well keep on producing during well tests. In contrast, the main disadvantage of this test is the difficulty to achieve well flow at constant rate.

Pressure build up tests are used widely in petroleum industry. In this test, the well is under a shut in condition after flow at constant rate. The major benefit of this test is the constant rate condition is easy to accomplish due to the flow rate is zero. Meanwhile, the drawback of the test is production loss since the well does not produce.

2.1.3. Injection and Fall-off Tests

Currently, water injection as a part of secondary recovery methods is widely used around the world. Well testing of injection wells becomes important to control water injection performance and to support further tertiary recovery projects. In injection tests, fluid flow into the well with constant injection rates and the pressure variation over time is measured. Following the injection test, the falloff test is conducted after the well is shut in.

The analysis of both tests can be linked with several problems if the injected fluid is different with original reservoir fluid such as water is injected in an oil zone for displacement. This problem can be solved when both tests are considered identical in terms of methods and solutions of analysis (Larsen, 2010). There are some cases where the result for both tests has different answers. It may be caused by induced fracture during injection phases.

2.1.4. Pressure Derivatives

In 1983, Bourdet *et al*. introduced the pressure derivative in regard to the time logarithm. It could be stated as a function of the time derivative and elapsed time (Δt) since the beginning of the flowing periods, given by:

$$\Delta P' = \frac{dp}{dln(\Delta t)} = \Delta t \frac{dp}{d\Delta t} \tag{1}$$

In shut-in periods following a single drawdown phase, the pressure derivative is generated based on the superposition time (effective Agarwal time), given by:

$$\Delta P' = \left(\frac{t_p \Delta t}{t_p + \Delta t}\right) \frac{dp}{d\left(\frac{t_p \Delta t}{t_p + \Delta t}\right)} = \left(\frac{\Delta t}{t_p + \Delta t}\right) \frac{dp}{d\left(\frac{\Delta t}{t_p + \Delta t}\right)} \tag{2}$$

In pressure transient analysis, the pressure change and derivative are plotted on log-log scales versus Δt.

2.1.5. Flow Regimes in Pressure Transient Test

In general, there are 3 major flow regimes emerge in pressure transient analysis which are transient, pseudo steady state, and steady state. Transient state is observed in the early time of pressure responses before it is affected by the influence of closed or constant pressure boundaries. The change of pressure over time is a representation of the well and reservoir parameters, e.g. permeability and fracture properties. Transient behavior is recognized as a main part of well test interpretations.

The pseudo steady state (PSS) regime is identified when closed (bounded) boundaries are reached while steady state flow is characterized by a condition when the pressure is constant over a period of time.

2.1.6. Interference Test

In interference tests, bottom-hole pressure responses of the observation well with shut in condition are analyzed corresponding to a production or shut-in phases of an active well. Theis (1935) proposed type curve for interference tests called line source solution in which represents the dimensionless of pressure p_D versus the dimensionless time-distance group t_D/r_D^2.

Theis presented following equation for pressure performance of the observation well in oil field units:

$$P_i - P(r,t) = \Delta P = 141.2\frac{q\mu B}{kh}P_D(r_D, t_D) \tag{3}$$

Where P_D are defined by:

$$P_D = -\frac{1}{2}Ei\left(\frac{-{r_D}^2}{4t_D}\right) \tag{4}$$

Also the time t_D/r_D^2 is:

$$\frac{t_D}{r_{D^2}} = \frac{0.000264k}{\phi\mu c_t r^2}\Delta t \tag{5}$$

In 1980, Tiab and Kumar recommended a derivative type curve for interference tests by the rate of pressure change with time and the time derivative is multiplied by Δt. Their model is identical with Theis solution. There are two main attributes for type curves of interference tests which are the periods when the derivative is higher than pressure change and after the two curves intersect following the start of radial flow (figure 2).

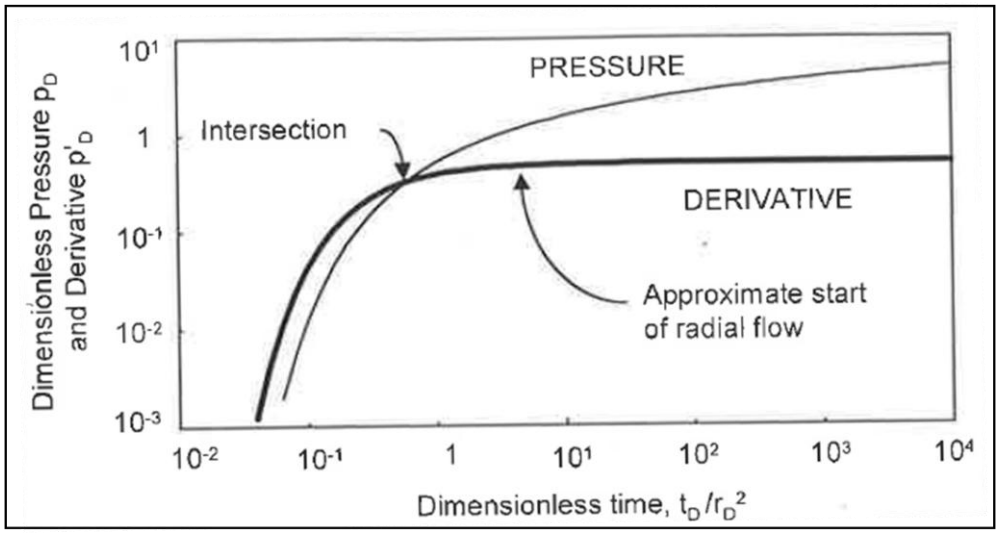

Figure 2: Log-log scales of Theis solutions. Pressure and derivative responses. (adapted from Bourdet, 2002)

In interference tests, the pressure and derivative curve of observation wells in log-log graph are simple and not a family of curve resulted from production or injection well tests (Bourdet, 2002).

The time for the pressure responses arrives on the observation well depends on the relative location between the wells, reservoir properties, and directional permeability towards the active wells (Bourdet 2002). In addition, Jargon (1976) explained the wells with stimulation treatments causing the response time to reach the observation well earlier compare with line source solution.

2.2. Hydraulic Fracturing

The hydraulic fracturing process, which was introduced to the industry in 1947, is caused by fluid pressure inside the rock exceeds the minimum principal stress along with the tensile strength of the rock (E.Fjaer *et al*. 2008). It is mainly used for increasing production rate of the well by pumping fracturing fluid into the formation at a high specific rate and pressure until rock failure.

Hydraulic fracturing has a significant contribution to enhance hydrocarbon reserves. Moreover, it has been used to increase injectivity and improve sweep efficiency in water injection treatment.

2.2.1. Fracture Orientation

The principal stresses in the subsurface formations and near wellbore are key factors governing the fracture orientation. Fracture planes extend hydraulically in the direction perpendicular to the least principal stress in the formation (Soliman *et al*. 1990). In

most cases, the minimum principal stress is in the horizontal direction causing the fracture plane to be vertical around a vertical borehole.

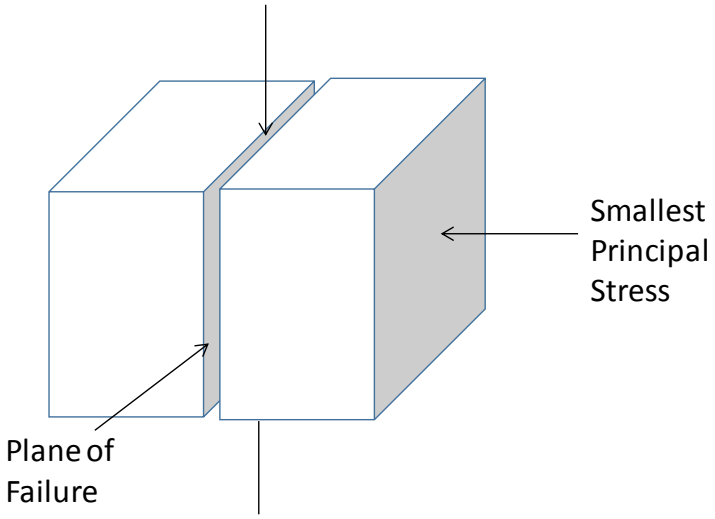

Figure 3: Fracture orientation in the vertical well

In horizontal or deviated wells, the direction of fracture propagation is more complicated to generate. When the smallest in-situ stress is parallel to the wellbore, the plane of fracture will be normal to the well, called a transverse fracture. Meanwhile, a longitudinal fracture whose plane is parallel to the wellbore is generated when the smallest in situ stress is perpendicular to the wellbore.

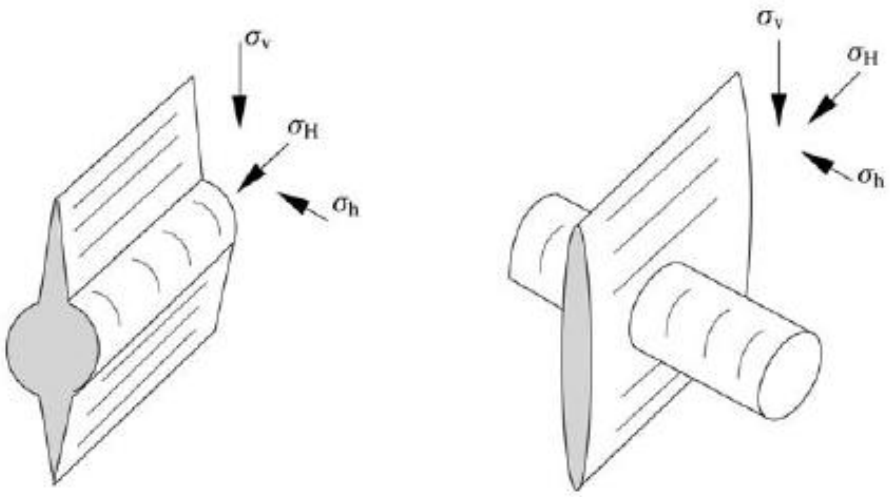

Figure 4: Fracture orientation in the horizontal well (adapted from E.Fjaer *et al.* 2008)

Studies by Larsen and Hegre (1994 b) and Soliman *et al*. (1996) concluded that horizontal wells with transverse fractures have higher potential productivity than horizontal wells with a longitudinal fracture for high conductivity fracture.

2.2.2. Fractured wells in well testing

There are three major models of the fracture in pressure transient behavior:

- Finite Conductivity Fractures
- Infinite Conductivity Fractures
- Uniform Flux Fractures

Finite conductivity fractures have constant properties (i.e. permeability and thickness within fractures) and also the pressure loss within fractures is not negligible. For this case, Cinco and Samaniego (1981) considered various flow regimes can be noticed with respect to time a) linear flow, b) bilinear flow and c) radial flow.

Fracture linear behavior is observed typically at early time and has a straight line with half-unit slope on a log-log plot of pressures and derivatives. As the time increase, bilinear flow corresponding with ¼ slope straight lines may or may not present following by formation linear flow, also with ½ slope. At the latest, pseudoradial flow phase is exhibit.

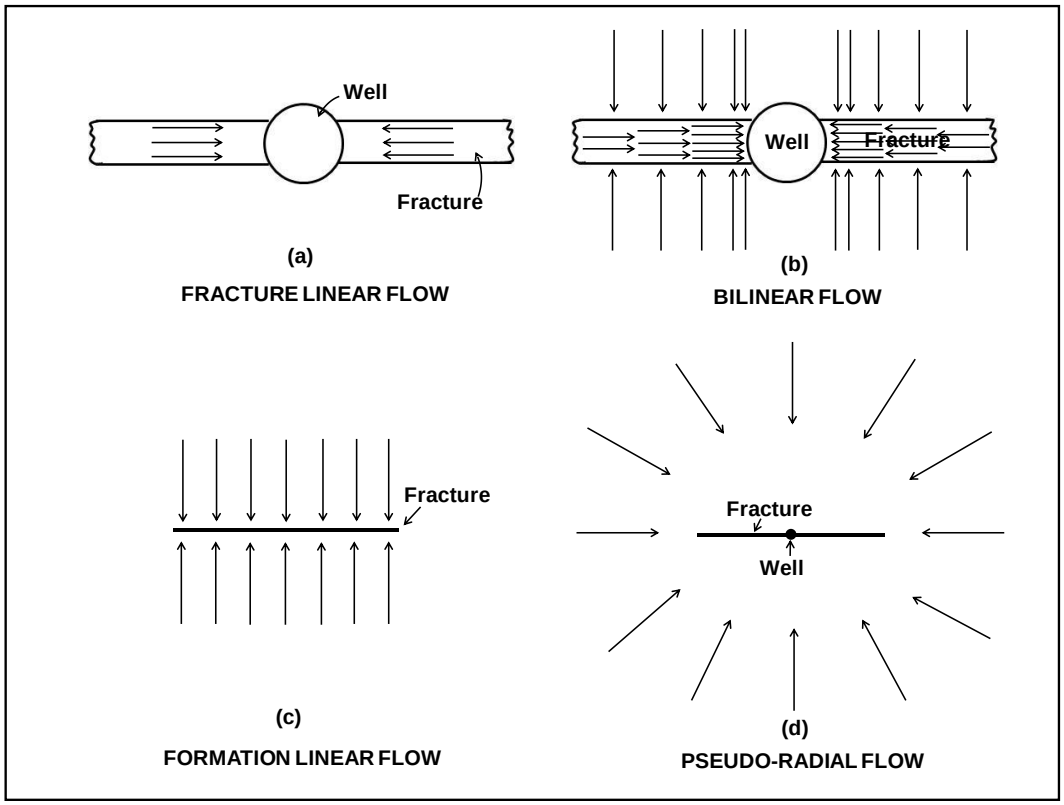

Figure 5: Flow regime in fractured wells (adapted from Cinco-Ley and Samaniego, 1981)

Infinite conductivity fractures are characterized by uniform pressure inside the fracture. This condition is fulfilled when fractures have very high permeability.

Gringarten *et al*. (1974) examined that the linear flow is a characteristic of pressure transient behavior of this fracture model.

Fractures with the pressure gradient distributed uniformly over the entire fracture length are known as uniform flux fractures. There is only a slight difference in flow behavior between infinite conductivity and uniform flux fractures.

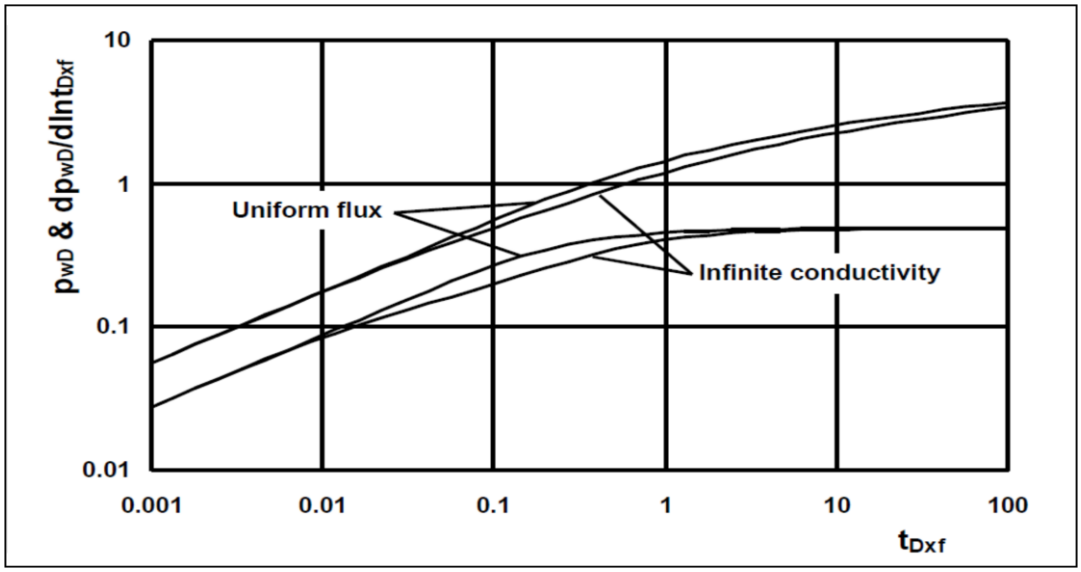

Figure 6: The comparison of pressure and derivative between uniform flux and infinite conductivity fractures. (adapted from Cinco-Ley and Samaniego, 1981)

2.2.3. Fractured Horizontal Well

Larsen and Hegre (1994 a) addressed fundamental flow periods for fractured horizontal wells with the assumption that the well is only perforated in the fractured segments. They concluded that transverse and longitudinal fractures are similar in the sense that both start with the fracture responding (radial flow for transverse fractures and linear and bilinear flow from longitudinal fractures) and followed by formation linear and pseudo-radial periods prior to reach boundary effect.

They also described that formation linear and bilinear periods may appear in the longer transverse fracture. In multi-fractured horizontal wells, the compound linear flow might be observed due to interference between fractures. This period appears after early radial phase where fracture flow independently without interference from neighboring fractures. The compound linear flow is depends only on the distance of the outer fractures and is independent of the number of fractures.

Chen and Raghavan (1997) explained that the surface of fracture should be related to the value of reservoir permeability (wide fractures in high permeability reservoirs and long fractures in low permeability reservoirs) and fracture spacing.

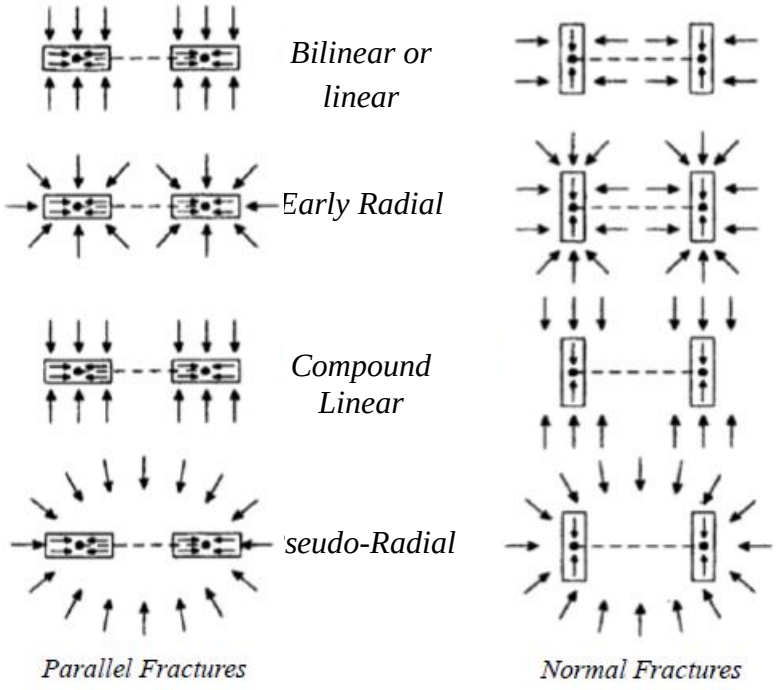

Figure 7: Type of flow regime in the horizontal well intercepted by fractures (adapted from Chen and Raghavan, 1997)

2.2.4. Determination of Fracture Orientation

In recent years, there are some techniques to ascertain fracture orientation. Elkins and Skov (1960) modeled how the orientation of fracture can be determined. Their analysis based on the assumption of natural fractures which perform such as an anisotropic system and used a line source calculation for the investigation.

Uraiet *et al.* (1977) developed an analytical solution to determine the orientation of a vertical fracture using an interference test. They showed how orientation of the observation well with respect to the fracture plane impacted a dimensionless pressure change of the observation well.

Cinco-Ley and Samaniego (1977) proposed mathematical models and provided a type curve of finite conductivity fractures in interference tests. Their model is an extension from Uraiet *et al.* (1977) method.

Meehan *et al.* (1989) developed a semi-analytical model for interference tests for finite conductivity hydraulic fractures. Their calculation based on flux distributions at observation and active wells to generate pressure outcomes in both wells.

Spencer and Chi (1989) introduced a seismic method for estimate fracture orientation. They assumed the reservoir characterized as an azimuthally anisotropic medium.

Another method to estimate fracture orientation is a pulse testing technique (Pierce *et al*. 1975, Tiab and Abobise, 1989).

2.2.5. Induced Fracture in Injection Well

Fractures might be induced hydraulically from injection wells when the bottom-hole pressure is higher than the pressure at which formation breaks. Induced fractures in injection wells can lead to increase recovery factor and cut operational cost (Husted *et al*. 2006). Some studies have been published and discussed how the geometry of induced fractures impact the areal sweep efficiency. It gives negative impact when the growth of induced fractures towards nearby production wells (Lacy, 1987).

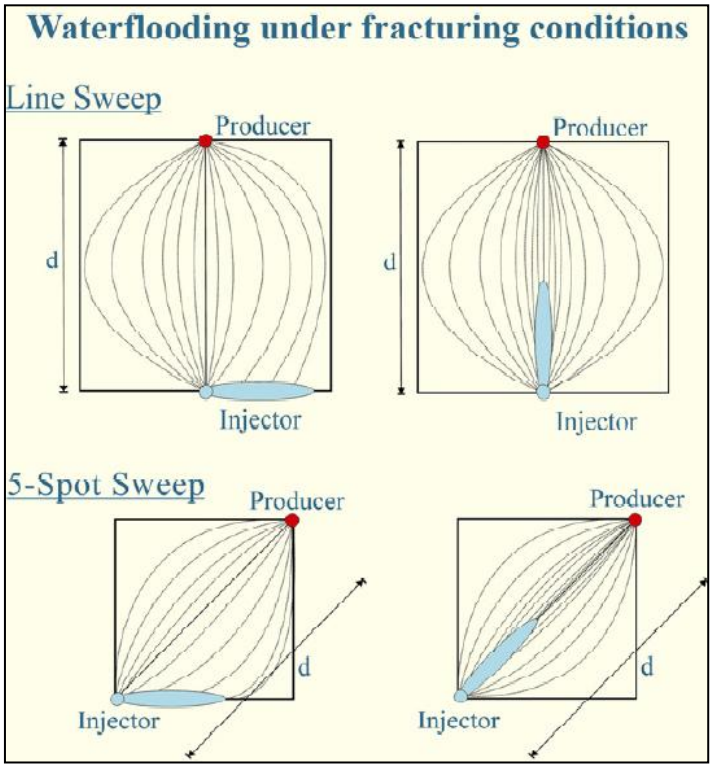

Figure 8: Impact of induced fracture direction on areal sweep (adapted from Husted *et al.* 2006)

Rod *et al*. (2005) introduced a new method namely FAST (Fracture Aligned Sweep Technology) applied for horizontal injection wells in densely spaced line drive waterflood. It is based on the fact that reservoir stresses is affected by fluid flow in low permeability reservoirs. This method ensures for longitudinal induced fracture situation and reduces the risk for early water breakthrough in nearby production wells by controlling the injection rate.

Figure 9: Illustration of FAST technique. Fracture induced in the injector well because of injection pressure (adapted from Rod *et al.* 2005).

2.3. Pressure (Stress) Dependent Permeability

Raghavan and Chin (2004) pointed out an approach to determine reduction in productivity as a result of pressure (stress) dependent permeability. By considering a fluid flow and geomechanical side, they developed correlations which quantified the change in Productivity Index (PI) as a function of mechanical parameters, overburden stress, well pressure, and area of drainage. One of the correlations is based on an exponential relationship between pressure (stress) and permeability change, defined as:

$$\frac{K}{K_i} = e^{-y_p(P_i - P)} \tag{6}$$

This correlation is used in this thesis to simulate a hydraulic induced fracture case.

3. Numerical Simulation and Analytical Well Tests

A software called a reservoir simulator is used to find a solution for multi-phase fluid flow equations. The reservoir simulation may integrate different input data including geological model, geophysical interpretations, petrophysics, well parameters, and surface facility constraints. It is a standard tool in oil and gas companies to make decisions on field development and possible investments.

In this thesis, numerical simulation study in combination with Pressure Transient Analysis (PTA) is used to give better understanding of geometry and dynamic parameters of induced fractures. Simulated downhole pressure data as a function of time resulted from the numerical simulation are further used for PTA interpretations. As a necessary step, a comparison of results from numerical simulations with analytical solutions available in the PTA tool is carried out. The purpose of the comparison is to match numerical simulation results by an analytical model if an equivalent analytical model may be assembled. Moreover a good match between responses from both methods will provide reliability of the analysis (Kamal *et al.* 2005, Shchipanov *et al.* 2014, and Egya *et al.* 2016). This is a starting point for the further interpretation of the numerical simulation results. Eclipse Blackoil Reservoir Simulator (E100) is used as numerical simulation software and Saphir as analytical PTA software.

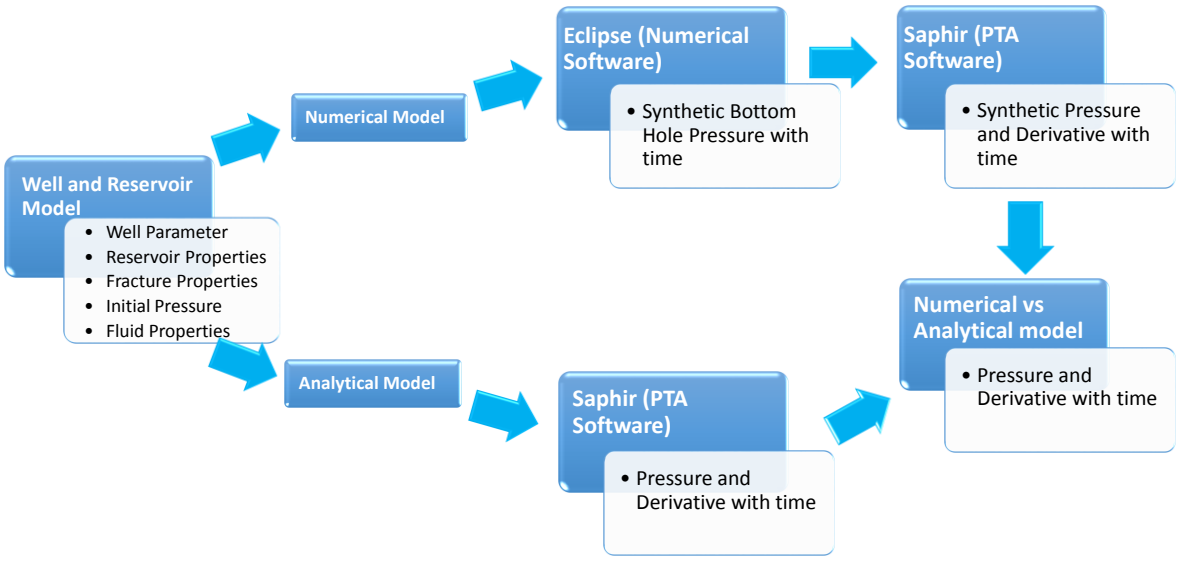

Figure 10: Workflow for combining numerical and analytical PTA

The explanation about all parameters and assumptions in numerical simulation and analytical models for various scenarios is presented in this chapter.

3.1. Simulation Model Description

A base model used for all cases is a homogeneous grid with rectangular shape and filled with 100% of water. The grid size and dimension are 20 feet and 50x250x10 respectively.

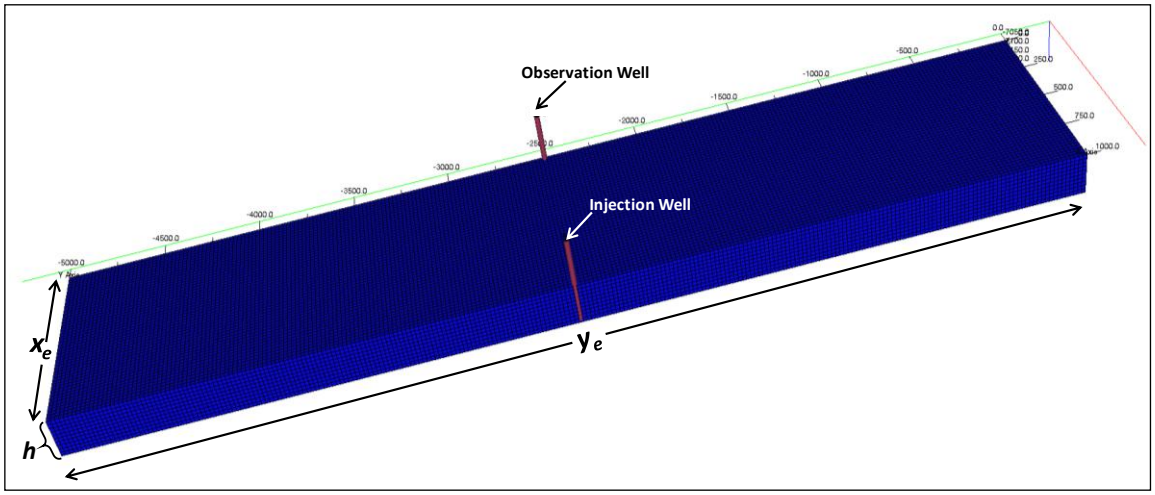

Figure 11: A reservoir model in numerical simulation

Two wells with open hole completion are used in the model, an injection well and an observation well. Both wells are placed at the corner grids of x coordinate and the centre of y coordinate therefore their rates only affect half of the model. In Eclipse, the well connection factor option (WPIMULT) should be used with value of 0.5. A simulation of single vertical injector without induced fracture is set as a base case. All reservoir and fluid parameters in the numerical simulation can be seen in table 1.

Table 1: Reservoir and fluid properties

Model length (y_e)	5000 ft
Model width (x_e)	1000 ft
Thickness (h)	200 ft
Porosity (ϕ)	0.3
Permeability (k)	1 md
Wellbore radius (r_w)	0.25 ft
Total compressibility (C_t)	0.00001 1/psi
Water viscosity (μ_w)	1 cp
Initial reservoir pressure (P_i)	4000 psi
Water formation volume factor (B_w)	1 RB/STB

3.2. Effect of Grid Size in Numerical Simulations

The output generated by numerical simulations is affected by the size of grid. Hegre (1996) have confirmed that the grid size has an impact on simulated pressure transients. Based on that reference, the grid size sensitivity is included to observe the effect to the pressure transient response. Three grid size scenarios are used consisting of grid size 10, 20, and 40 feet with the size of the reservoir kept constant.

As can be seen in figure 12, the grid size has an impact only in the early period of pressure and derivative responses. The slope of straight line (m) in pressure derivatives is one representing a grid block storage effect. As the size of grid is reduced, the grid storage periods will end earlier. After this period, there is no impact on the pressure and derivative for three scenarios of the grid size.

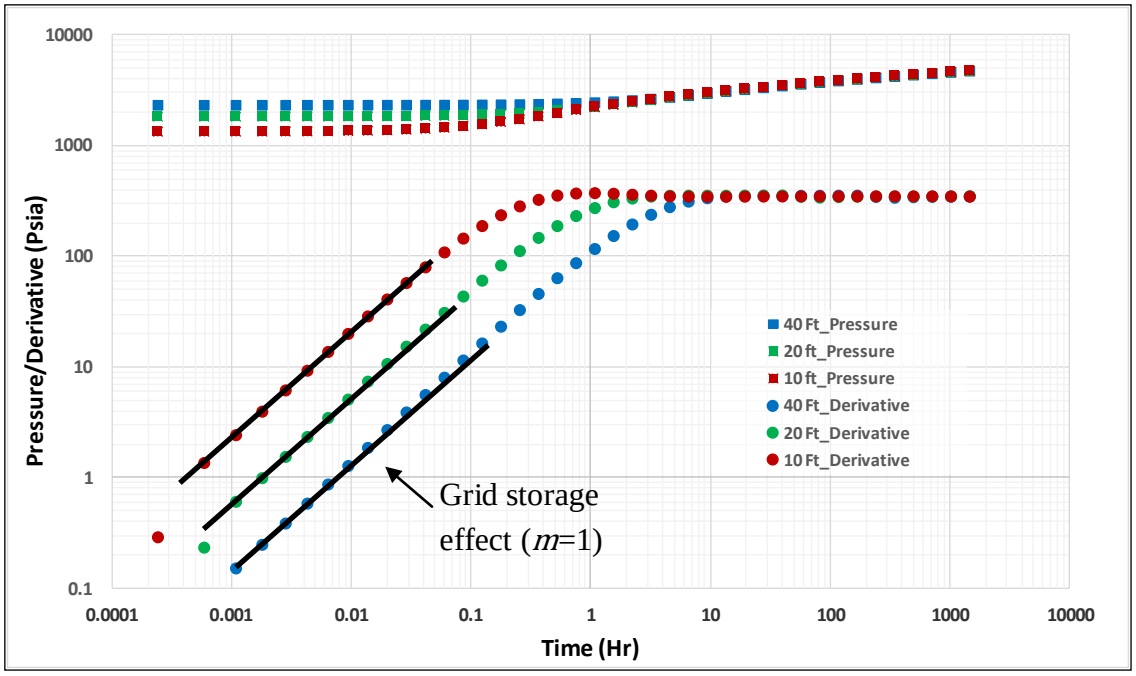

Figure 12: Synthetic pressures and derivatives for vertical well injector. Sensitivity on the grid size

3.3. Fracture Grid Block

In this thesis, fracture is defined as "induced fracture" in the injection well and "fracture" in the observation well. All fracture cases are using a fracture grid block represented by the fracture direction permeability.

To reduce a higher amount of the simulation time and computer memory capacity for fractured model cases, 20 ft is chosen as the main grid size and Local Grid Refinement (LGR) is introduced within the fracture grid block.

A gradual LGR (figure 13) is utilized to define the fracture width and avoid numerical error due to large change in the local grid size. Small size of the width of fracture grid block causes a numerical stability problem and increasing in the simulation time (Hegre, 1996). Therefore, 1 ft is chosen as the width of fracture grid block in order to reduce that problem.

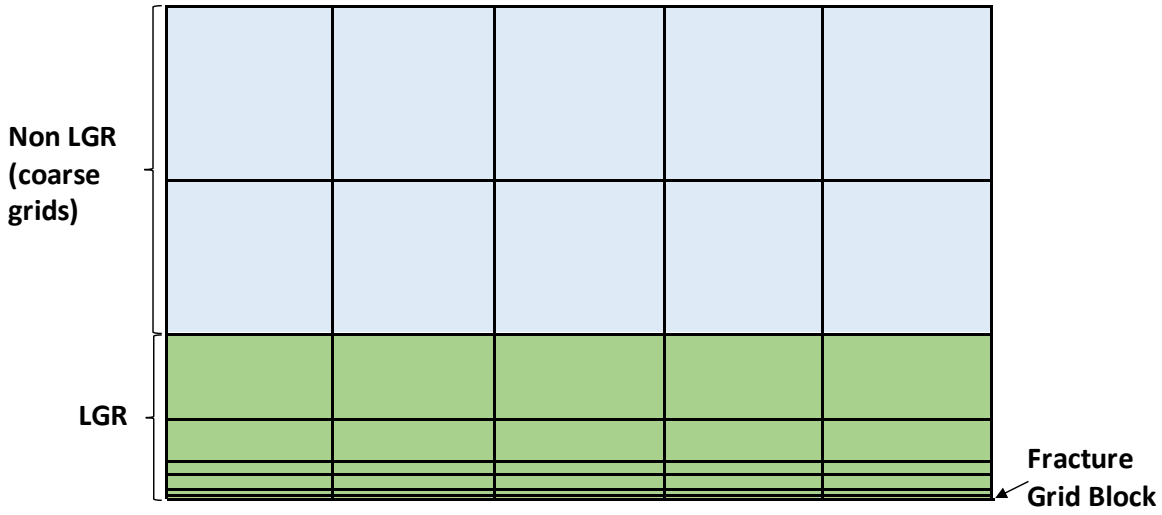

Figure 13: Gradual LGR in fracture grid block

A sensitivity study of fracture conductivity including 250, 2500, 25000, and 250000 md-ft is simulated to observe its effects on the fracture. As a brief note, the LGR is only used in a fracture grid but not used in other grids (without fractures). It might lead a grid block storage representing a "wellbore storage" at initial flow either in non fracture cases or in several induced fracture cases where some well sections connect directly to coarse grids.

3.4. Numerical Simulation of Well Test Scenarios

This thesis investigates two scenarios of well tests: single-well tests and interference tests. Both tests are divided into two periods, 60 days of injection periods with constant rate of 500 STB/day followed by the same duration of shut-in (fall-off) periods. These tests are simulated at increasing logarithmic time in Eclipse to get a good match with analytical solutions (Kamal *et al*. 2005 and Egya *et al*. 2016). The bottom-hole pressure generated by numerical simulations is analyzed and interpreted using Saphir (PTA software).

3.4.1. Single Well-Test Scenarios

This scenario carries out the simulation of well test in a single injection well. This test is subdivided into three scenarios based on various well geometries and induced fracture orientations.

Scenario 1: non-fractured wells

First scenario examines the effect of well geometry on pressure transient responses for a non-fractured well with the following cases:

- Base case : Simulation of a vertical injection well
- Simulation case 1 : Simulation of a horizontal injection well

The length for the horizontal well in all scenarios is 1000 meter and the distance from horizontal section to lower boundary (z_w) is 100 meter (see figure 14).

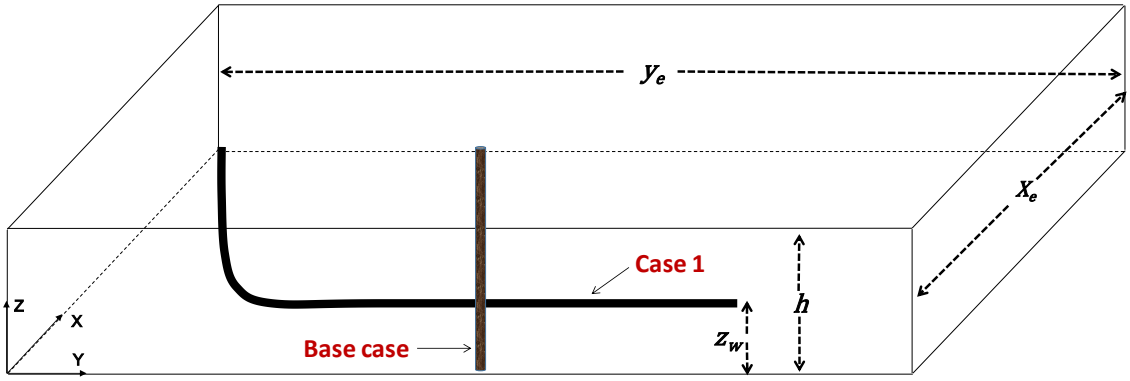

Figure 14: Injection well location

Scenario 2: fractured vertical wells

Two fracture orientations are implemented to study the impact of induced fracture geometry in the vertical well with cases:

- Simulation case 2 : a vertical injection well with induced fracture plane parallel to Y direction
- Simulation case 3: a vertical injection well with induced fracture plane perpendicular to Y direction

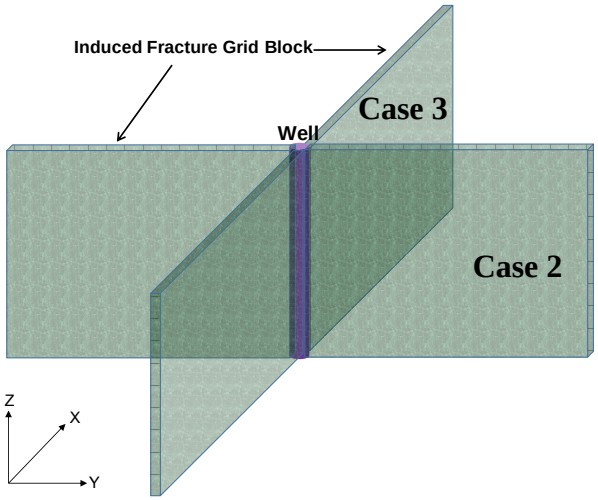

Figure 15: Model illustration of induced fracture direction parallel (blue) and perpendicular (green) with Y coordinate

Direction of the induced fracture is specified by the value of directional permeability in the fracture grid block. Table below shows induced fracture properties for case 2 and 3.

Table 2: Induced fracture properties. Case 2 and case 3

Parameter	Case 2	Case 3
k_x , mD	1	250000
k_y , mD	250000	1
k_z , mD	1	1
Half length (x_f), ft	500	500
Induced fracture height (h_f), ft	200	200

Scenario 3: fractured horizontal wells

This scenario investigates the impact of induced fracture geometry intersecting a horizontal injection well with cases as follow:

- Simulation case 4: a horizontal injection well with longitudinal induced fracture (parallel to horizontal well section)
- Simulation case 5: a horizontal injection well with single transverse induced fracture (perpendicular to horizontal well section)
- Simulation case 6: a horizontal injection well with multiple transverse induced fractures (4 induced fractures)

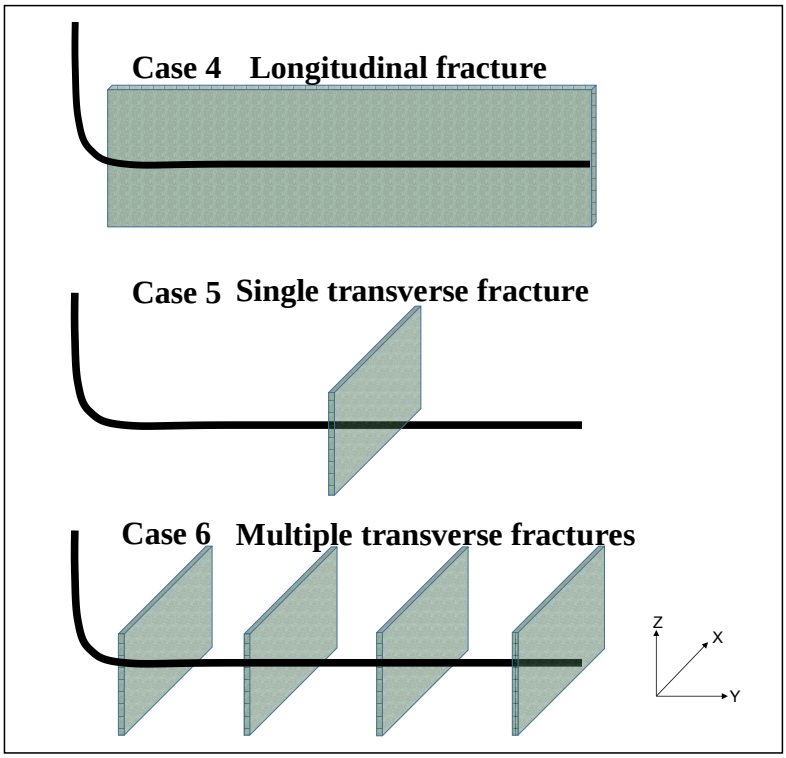

Figure 16: Fractured horizontal wells in numerical simulations

In case 5, fracture is placed in the center of horizontal well. All cases in this scenario have equivalent fracture surface where half length for case 4 and 5 is 500 ft and case 6 is 125 ft. For case 6, there are 4 transverse induced fractures with the total fracture half length is 500 ft and distances between neighboring fractures are uniform. Details property for fracture grid block in this scenario could be seen in table 3.

Table 3: Induced fracture properties. Case 4, case 5 and case 6

Induced Fracture Properties	Case 4	Case 5	Case 6
K_x , mD	1	250000	250000
K_y , mD	250000	1	1
K_z , mD	250000	250000	250000
Half Length (x_f), ft	500	500	125
Fracture Height (h_f), ft	200	200	200
Number of Fracture	1	1	4
Distance between neighboring fractures ($\boldsymbol{y_f}$), ft	-	-	312.5

For further analysis of case 6, impact of the distance between neighboring induced fractures is included in this scenario. The dimensionless of fracture half length is used to investigate this study with following formula:

$$y_{fD} = \frac{Distance\ between\ neighboring\ fractures\ (y_f)}{Fracture\ half\ length\ (x_f)} \quad (7)$$

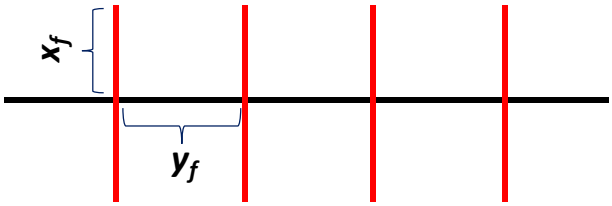

Figure 17: Illustration of multi transverse induced fractures

Previously, y_{fD} for case 6 is 2.5, the extreme case with y_{fD}= 0.5 is applied to observe the difference in pressure transient responses.

3.4.2. Interference Test Scenarios

Now, we introduce multi well tests technique by adding one well acting as an observation well namely interference tests. The observation well is shut-in but the perforation is open therefore it is possible to interpret the bottom-hole pressure change.

Many interference field tests are performed when the observation well is fractured (Mousli *et al*. 1982). To mimic the field application, a horizontal observation well with a longitudinal fracture is selected. It is placed at the corner of x coordinate and opposite with an injection well (Figure 18).

It should be noted that this study does not examine the effect of well and fracture geometry of the observation well on pressure transient responses as had been studied by Mousli *et al*. (1982). The grid size may influence the pressure response time on the observation well. Table 4 shows the observation well and fracture geometries in this scenario.

Table 4: Observation well parameters

Distance to active well (x_i)	1000	ft
Well radius (R_w)	0.25	ft
Fracture permeability (k_f)	250	Darcy
Fracture half length (x_f)	500	ft
Z_w	100	ft
Type Of fracture	Longitudinal	

The simulation of interference tests subdivided into two scenarios based on various well and fracture geometries intercepting the injector and one scenario which simulate hydraulic induced fracture from the injection well.

Scenario 4: interference tests for non-fractured injection wells

For this scenario, two cases are used to help give better understanding about impact of well injection geometry on pressure transients of the observation well. Those cases are:

3. Simulation Case 7: Interference test for a vertical injection well.
4. Simulation Case 8: Interference test for a horizontal injection well.

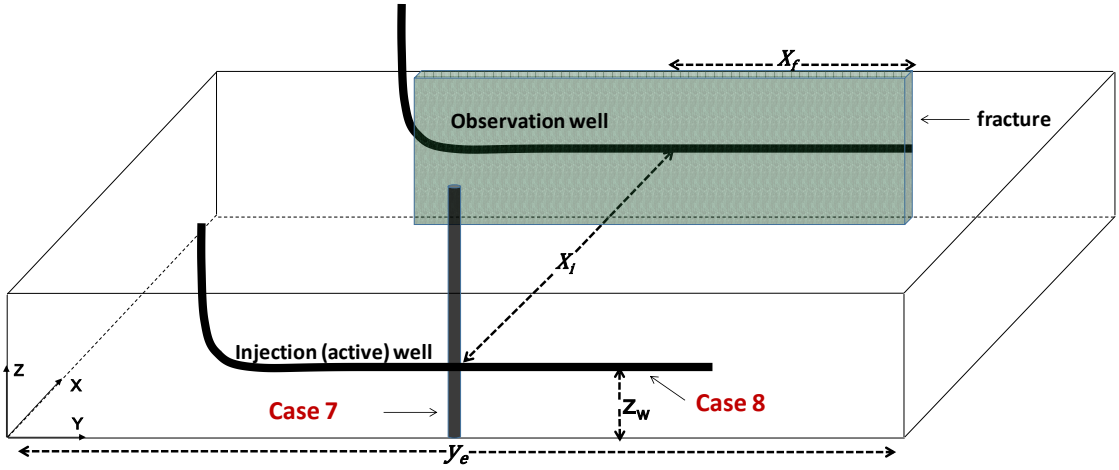

Figure 18: Model illustration for interference test of non-fractured vertical and horizontal injection wells in numerical simulation

Scenario 5: interference tests for fractured horizontal injection wells

This scenario investigates an interference test for two fracture geometries in scenario 3, longitudinal and single transverse fracture and observes the differences on pressure transients of the observation well. These cases are:

- Simulation case 9: interference test of a horizontal injection well intersected by a longitudinal induced fracture
- Simulation case 10: interference test of a horizontal injection well intersected by a transverse induced fracture

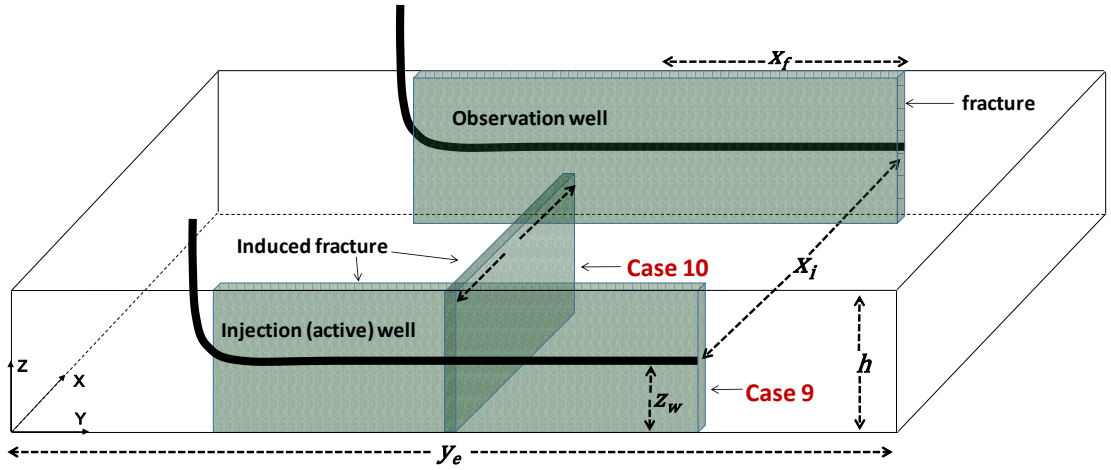

Figure 19: Model illustration for interference test of fractured horizontal wells in numerical simulation

Scenario 6: Simulation of hydraulic induced fracture in interference tests

For some fields with waterflood scenario, fractures are hydraulically induced when pressure around wellbore is higher than the fracture pressure (see section 2.2). Here is a scenario represented that case by applying pressure dependent permeability, $k_f(p)$, within induced fracture grid block and observing the impact on pressure transients of the observation well.

The induced fracture grid block intersecting an injection well has similar value with matrix permeability (1 md) at initial pressure. When pressure increase, permeability of fracture will change based on permeability modulus model from Raghavan and Chin (2004). Fracture permeability of 250 darcy is set at the highest pressure observed in case 8 (figure 20). In addition, fracture permeability is defined similar with non-fractured grid below initial pressure. With these boundaries, the value of y_p should be 0.0086 (figure 21).

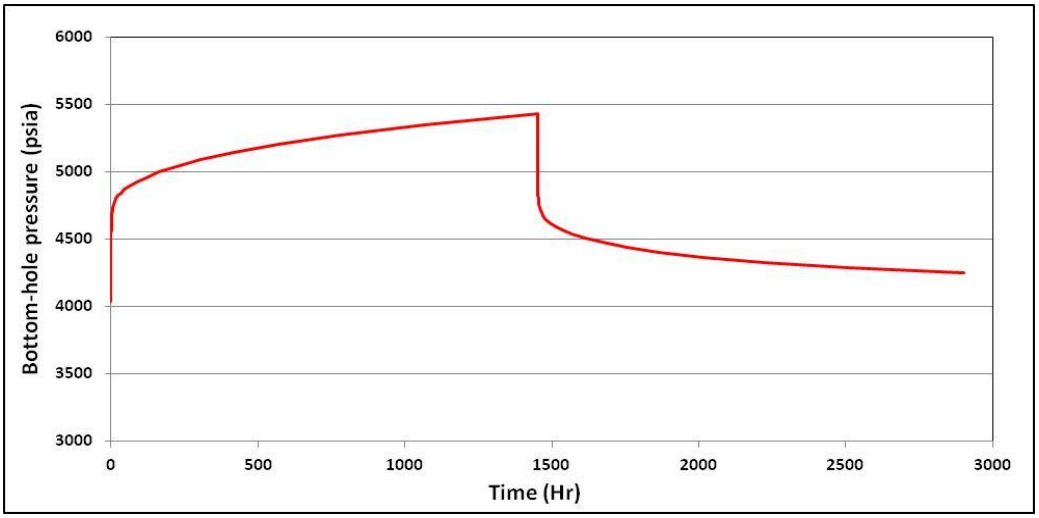

Figure 20: Simulated bottom-hole pressure (non fractured horizontal well case)

Simulation of pressure dependent fracture permeability in Eclipse employs two following keywords:

- ROCKTAB (Rock Compaction Data Tables) to generate transmissibility multipliers as a function of pressure.
- ROCKCOMP (Rock Compaction Option) have a function to enable pressure dependent transmissibility multipliers and pore volume.

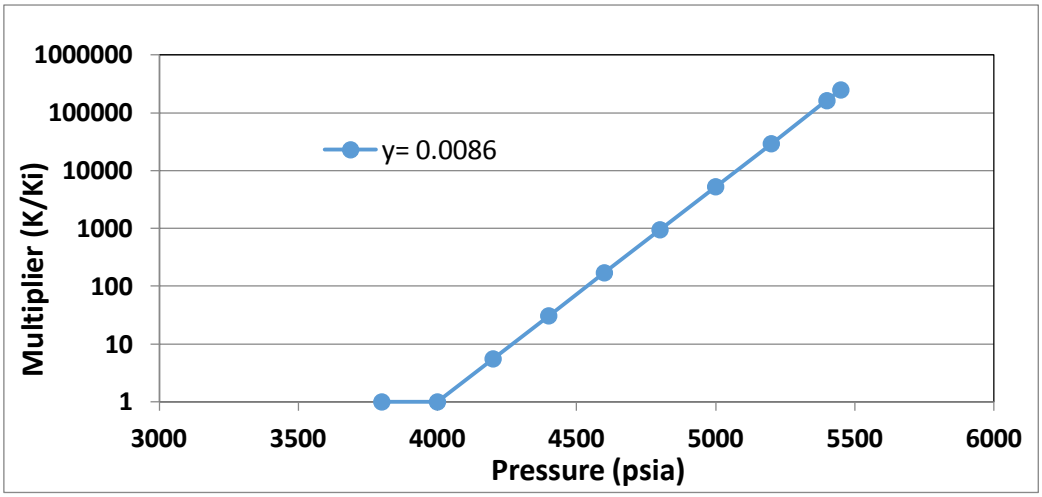

Figure 21: $k_f(p)$ plot

Two cases in scenario 6 are implemented with following cases:

- Simulation case 11: a longitudinal induced fracture with $k_f(p)$. k_y and k_z in fracture grid block is pressure dependent while k_x is constant (table 5)
- Simulation case 12: a transverse induced fracture with $k_f(p)$. k_x and k_z in fracture grid block is pressure dependent while k_y is constant (table 6)

Table 5: Pressure dependent fracture permeability for a longitudinal fracture case (ROCKTAB)

Pressure	Pore Volume	Trans-X	Trans-Y	Trans-Z
3800	0.999	1	1	1
4000	1.000	1	1	1
4200	1.001	1	5.6	5.6
4400	1.002	1	30.8	30.8
4600	1.004	1	171.1	171.1
4800	1.005	1	949.6	949.6
5000	1.006	1	5271.1	5271.1
5200	1.007	1	29260.7	29260.7
5400	1.008	1	162429.6	162429.6
5450	1.009	1	249321.9	249321.9

Table 6: Pressure dependent fracture permeability for a transverse fracture case (ROCKTAB)

Pressure	Pore Volume	Trans-X	Trans-Y	Trans-Z
3800	0.999	1	1	1
4000	1.000	1	1	1
4200	1.001	5.6	1	5.6
4400	1.002	30.8	1	30.8
4600	1.004	171.1	1	171.1
4800	1.005	949.6	1	949.6
5000	1.006	5271.1	1	5271.1
5200	1.007	29260.7	1	29260.7
5400	1.008	162429.6	1	162429.6
5450	1.009	249321.9	1	249321.9

3.5. Analytical Well Test Scenarios

When an analytical well test model is generated, the information including well radius, thickness, porosity, permeability, total compressibility, and water viscosity are needed. Those properties should be similar with numerical simulation properties.

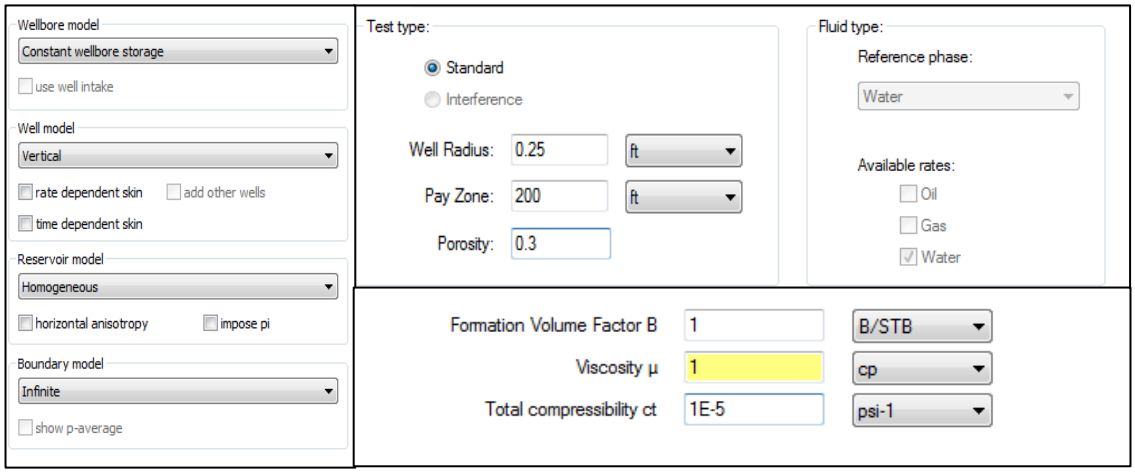

Figure 22: Reservoir and well initialization in PTA tool (Saphir)

Furthermore, the analytical solution is generated with the initial pressure and boundary parameters identical with numerical simulations. It employs a rectangle model as a representation of a sector model case in Eclipse software. Skin and wellbore storage are zero both in numerical and analytical models.

Parameter		Value	Unit	Pick
Well & Wellbore parameters (Tested well)				
C		0	bbl/psi	
Skin		0		
Reservoir & Boundary parameters				
Pi		4000	psia	
k.h		200	md.ft	
S	No flow	1000	ft	
E	No flow	2500	ft	
N	No flow	1000	ft	
W	No flow	2500	ft	

Figure 23: Well and reservoir parameters in analytical PTA

Study of analytical single-well tests uses three models to compare and combine with numerical simulations which are:

1. Vertical well model without fracture
2. Horizontal well model without fracture
3. Infinite conductivity fracture in vertical well model.

Analytical interference test

The line source method for analytical calculation (explained in section 2.1.6) is utilized to compare with various scenarios of simulated interference tests. The well and reservoir parameters ought to be similar with the numerical simulation. Skin and wellbore storage are zero despite there is a grid size compressibility effect in the numerical simulation.

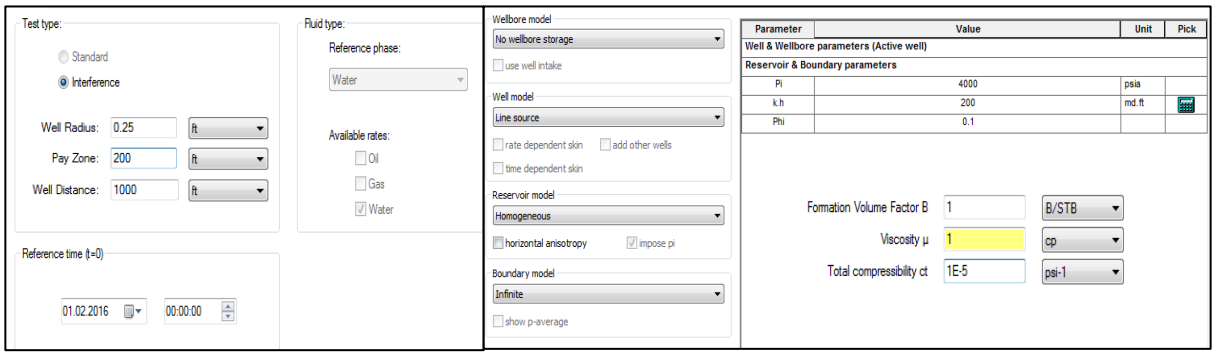

Figure 24: Reservoir and well parameters in saphir interference tests

4. Results and Discussion

In this chapter, results of all scenarios are presented, compared, and subsequently used to analyze and observe the differences in pressure transient responses. Details of the parameters and assumptions in all analytical and numerical simulations had been explained in chapter 3.

4.1. Single-Well Tests

The aim of single-well tests is to examine the differences in pressure transient behavior of vertical and horizontal injection wells intercepted by various induced fracture geometries (i.e. fracture orientation). The starting point in this study is combine numerical simulations and analytical models in order to get a good match in base case model (non-fracture wells)

4.1.1. Comparison between Analytical and Numerical simulations in Non Fractured Well

In figure 25, the pressure and derivate as a function of time resulted from numerical simulations and analytical solutions in injection and fall-off periods show a satisfactory match, given same well and reservoir properties in the two methods. It is noticed that coarse grids without local grid refinement (LGR) that were used in non fractured well cause the grid block storage effect in the early numerical result.

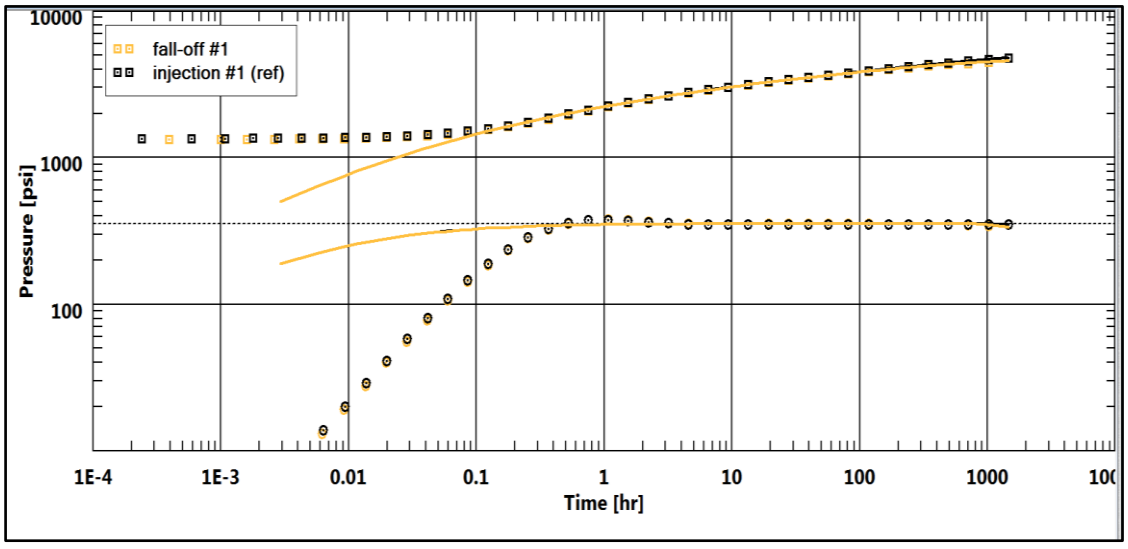

Figure 25: Comparison of analytical (line) and numerical (marker) simulations for base case

Figure 26 presents the good match between bottom-hole pressures versus time obtained from numerical simulations (dots) and analytical models (red line) in injection and fall-off periods.

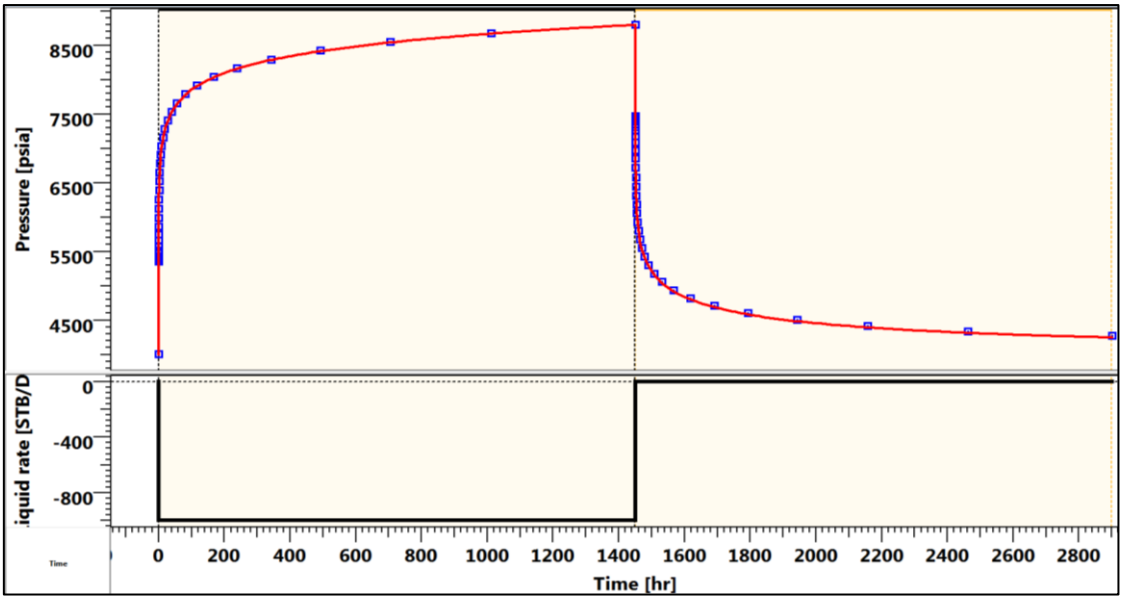

Figure 26: Analytical (dots) and numerical (line) responses, rate and pressure for base case

In a horizontal well case, both calculations also have similar results in injection and fall of periods (Picture 27). After grid block storage period, the flow regime is a radial phase represented by zero slope of straight line. After 40 hour, the pressure perturbations reach upper and bottom boundary and linear flow period is exhibited, denoted by half-unit slope log-log straight line.

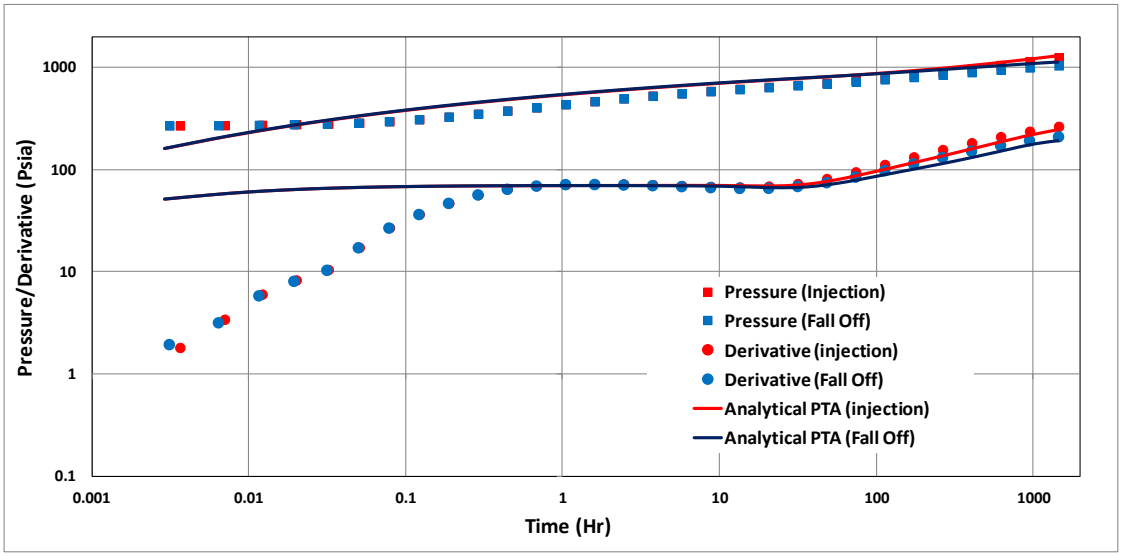

Figure 27: Pressures and derivatives for case 1. Injection and fall-off phases

In cases where fracture is not present, a good match between the analytical model and the numerical simulation is achieved demonstrates that both methods are reliable for interpretation of reservoir parameters, i.e. permeability.

4.1.2. Effect of Fracture Conductivity on PTA Responses

Flow regime in fracture is mainly influenced by the fracture's conductivity. A sequence of bilinear flow followed by linear formation and radial flow are characterizations of finite conductivity fracture while infinite conductivity fracture only have linear flow followed by radial flow (section 2.2.2). Figure 28 shows the pressure and derivative responses for induced fracture in a vertical well (case 2) for different fracture conductivity (250, 2500, 25000, and 250000 md-ft).

In low conductivity induced fracture, pressure derivative responses shows full of bilinear flow (¼ slope) for 250 md-ft and bilinear flow in early time continued with a linear formation flow (½ slope of straight line) for 2500 md-ft. For 25000 md-ft induced fracture, there is a short period of bilinear flow in the early time continued with linear flow.

In high conductivity induced fracture (250000 md-ft), only linear flow is observed representing an infinite conductivity fracture type. Thus, in order to represent infinite conductivity fracture, fracture conductivity of 250000 md-ft is used in all fracture scenarios.

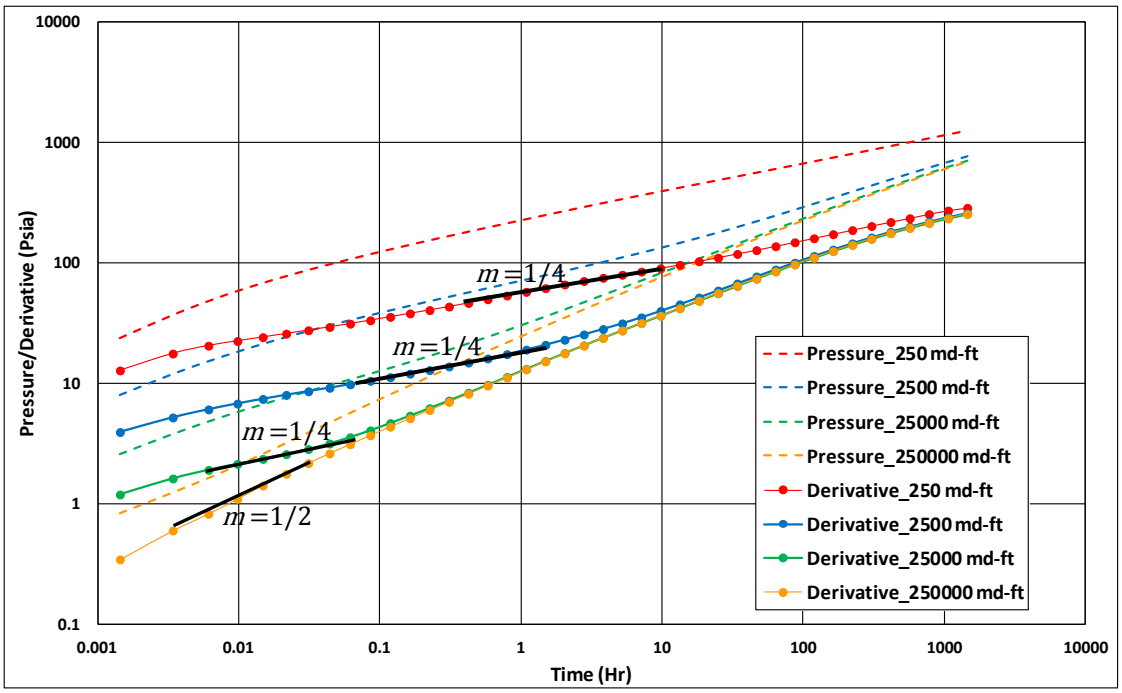

Figure 28: Figure 4.4: Impact of fracture conductivity in the fractured vertical well. Pressures (dashed line) and derivatives (line with marker)

4.1.3. Effect of Induced Fracture Direction in Vertical and Horizontal Wells

The pressure and derivative response for Case 2 and 3 as well as result from the analytical well test in injection and fall off phases are shown in figure 29. The

analytical model used in all fractured well cases was that of a vertical well with infinite conductivity fracture. The simulation of well test for case 2 and case 3 display comparable results with the analytical solution indicates that the numerical simulation is in line with the analytical model for fractured vertical well case. The straight lines with half slope characterize the fracture flow (linear) during pressure propagation.

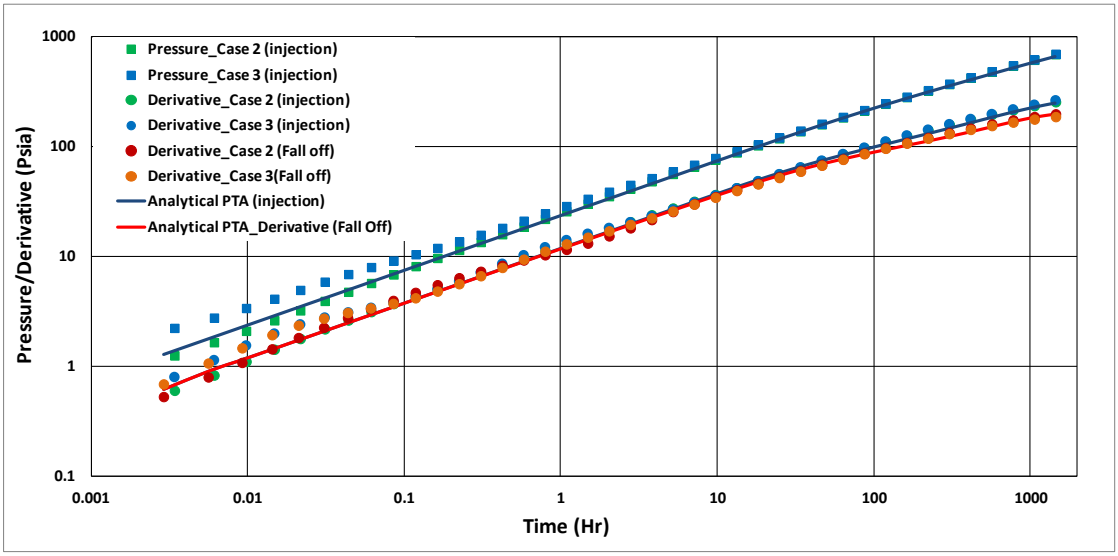

Figure 29: Pressures and derivatives for case 2 and case 3. Injection and fall-off phases

There is a slight difference in derivatives between injection and fall-off phases at the late time. It is caused by the logarithmic superposition scheme in fall-off periods. The derivative curve is a function of superposition time in shut-in periods (see section 2.1.4). Therefore when Δt is higher following long injection and fall-off periods, the pressure derivative curve may respond differently between both periods.

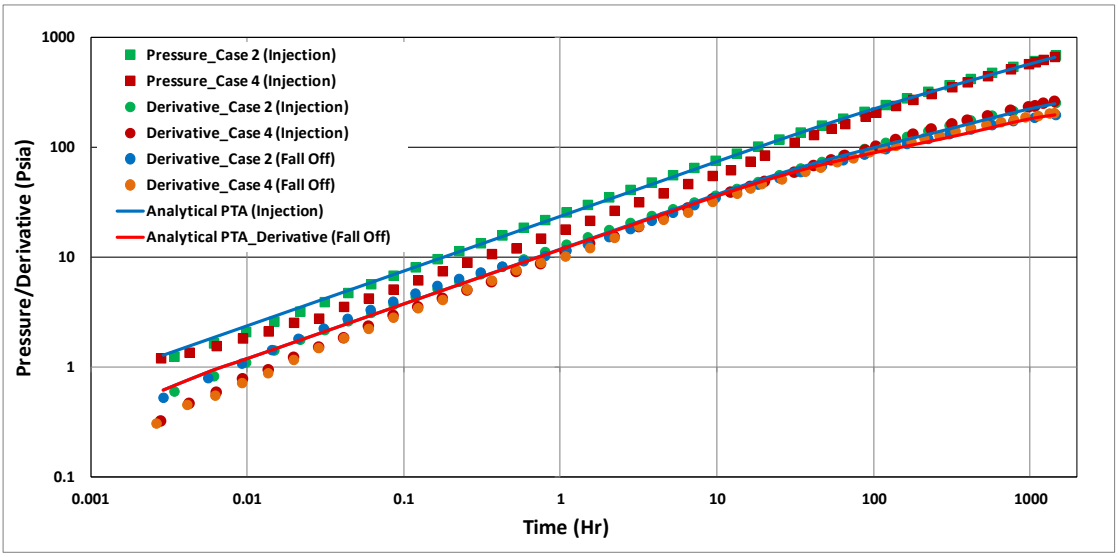

Figure 30: Pressures and derivatives for case 2 and 4. Injection and fall-off phases

Graph in figure 30 explains that the response in case 4 is identical with case 2 and both cases are satisfactory match with analytical solution of infinite conductivity fracture intersecting a vertical well. Correspondingly, only linear flow occurs at longitudinal (parallel) induced fracture intersecting a horizontal well. The fall-off and injection periods have similar result except at the late time period.

Based on these results, it can be concluded that case with longitudinal (parallel) induced fracture intersecting a horizontal well (case 4) has similar pressure transient responses to the case of induced fracture intersecting a vertical well (case 2 and case 3). This conclusion can be explained based on the reference presented by Larsen (1998). All points within infinite conductivity fractures have uniform pressure. Accordingly, in the case with a vertical well intercepted by the infinite conductivity fracture and a horizontal well intercepted by the longitudinal (parallel) infinite conductivity fracture, the fracture and the perforated well sections can be treated as well elements (figure 31). The skin factor of the well element for case 2, case 3, and case 4 with equivalent fracture surface area is similar. It can be estimated by following equation (Larsen, 1998):

$$s = ln\frac{2r_w}{x_f} - \frac{h}{x_f} ln\left(sin\frac{\pi h_f}{2h}\right) \quad (8)$$

Therefore, the pressure response for those cases will be similar and the linear flow to the induced fracture will be not affected.

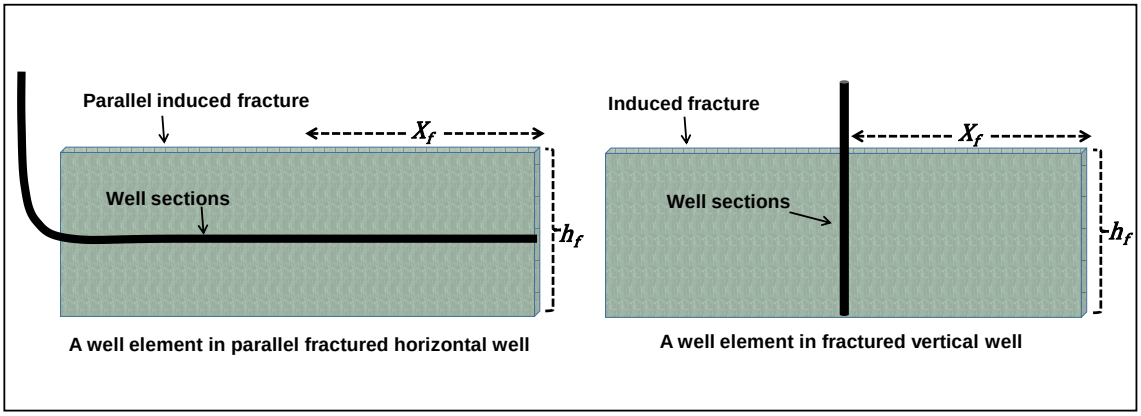

Figure 31: Illustration of well elements in a well with infinite conductivity fracture

Figure 32 displays the comparison between pressure change versus time from longitudinal induced fracture (case 4), single transverse induced fracture (case 5), and multiple transverse induced fractures (case 6). In the early time pressure build-up around the wellbore is higher for transverse induced fracture cases than longitudinal induced fracture case. It should be noted that the horizontal well section connected to coarse grids have an impact to simulated pressure and derivative responses at initial

time (section 3.3). Therefore, the differences on pressure build-up at initial time may be caused by the grid size effect.

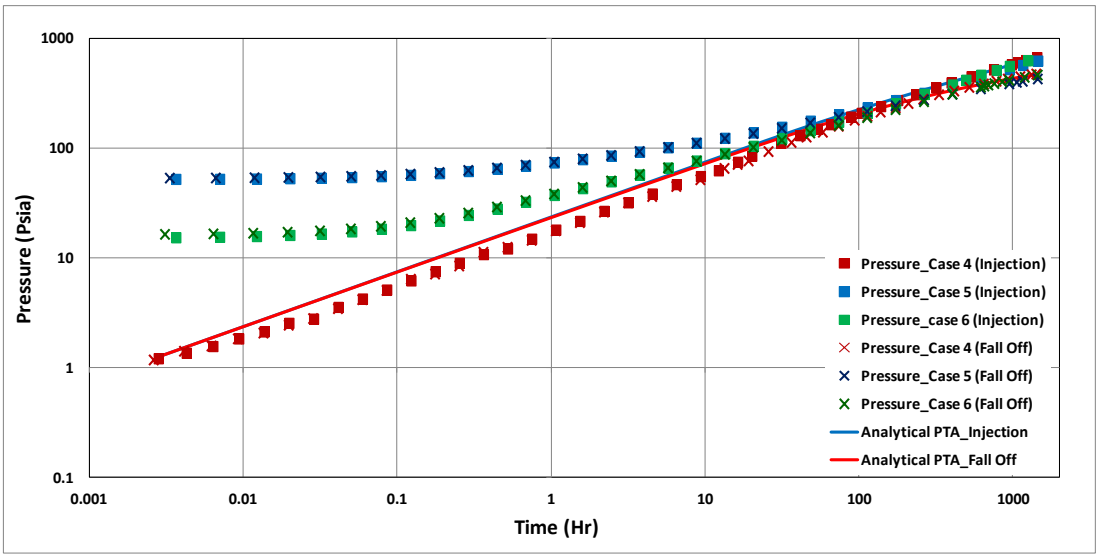

Figure 32: Pressures for case 4, 5 and 6. Injection and fall-off phases

An examination of figure 33 shows that the derivative between longitudinal induced fracture and single or multiple transverse induced fractures have similar behaviors that are characterized by half slope of straight line (linear flow). Hence, it can be concluded that the fracture orientation intercepting the horizontal well do not affect the linear flow to the fracture.

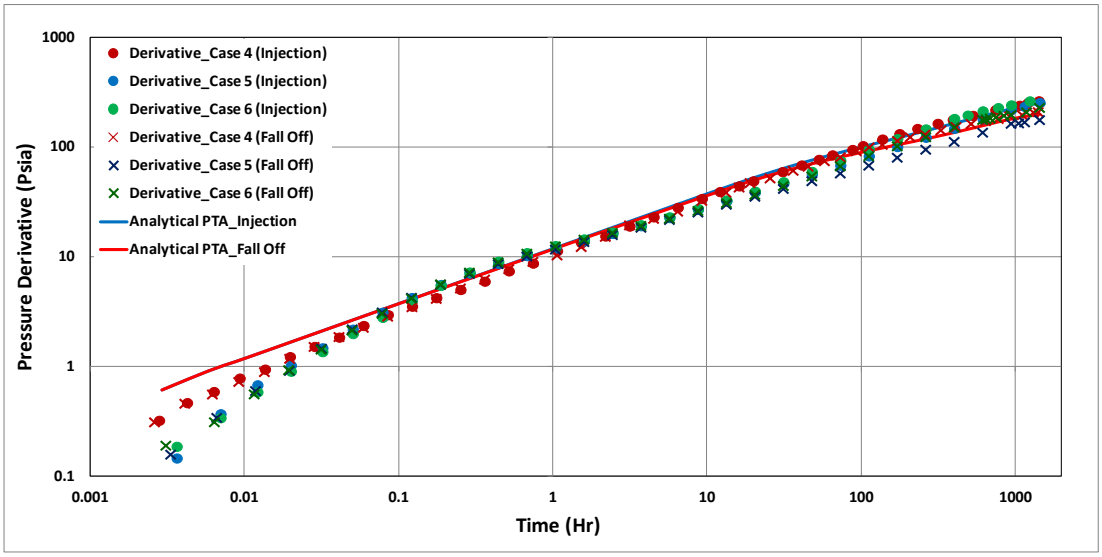

Figure 33: Pressure derivatives for case 4, 5 and 6. Injection and fall-off phases

This section point out how the simulation of single-well test is capable to generate synthetic pressure transients from various well and fracture geometries. Furthermore, a good match between responses from numerical simulations and analytical models

confirms capabilities of analytical well tests in interpreting pressure transient responses from cases with distinct well geometries and fracture orientations.

4.1.4. Impact of Fracture Distance in Multiple Transverse Fracture Case

The outcome from previous induced fracture scenarios show no unique pressure derivative is observed from the two cases of induced fracture orientation intercepting either horizontal or vertical wells. Now, a further examination of fracture distance in multiple transverse induced fractures is presented to detect a particular derivative response in that case.

From figure 34 it can be seen that the compound linear regime represented by higher slope of straight line (half slope) is occurred after 4 hour in case of y_{fD} = 0.5. The flow regime is caused by interference flow between fractures as the distance of neighboring fractures are getting shorter. By increasing the distance between neighboring fractures five times, the interference effect is vanished.

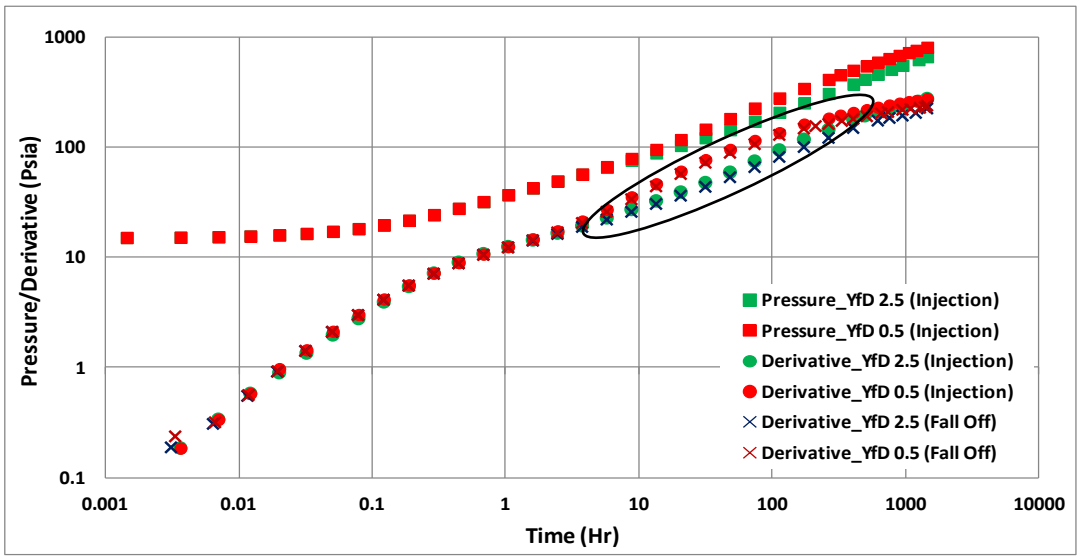

Figure 34: Effect of fracture distance in multiple transverse induced fractures. Injection and fall-off phases

Larsen and Hegre (1994 a) have previously conducted an analytical study about the effect of fracture distance in multiple transverse fractures and longitudinal fractures. Their investigation showed that a compound formation linear flow may occur when the distance between fractures are shorter.

Based on results from the author's numerical study and a reference from previous analytical calculations, it can be summarized that it is possible to detect whether the well is intercepted by multiple or single induced fracture if the distance between each fractures is relatively close.

4.1.5. Conclusion of Single-Well Tests Study

Well tests for various induced fractures and well geometries were simulated to observe the differences in pressure transient profile with respect to time. Analytical models are included to compare and confirm the numerical simulation results. Based on the results and comparison for some cases, interesting observations are given as below:

1. The grid size in the numerical simulation only affect at initial time of pressure transient responses.
2. Good match in pressure transient responses between numerical and analytical simulations verify both methods are reliable for the analysis. (figure 25, 26, 27, and 29).
3. Infinite conductivity fracture characterized by full linear flow is accomplished for induced fracture with conductivity 250000 md-ft (figure 28).
4. Vertical and horizontal wells intercepted by same direction of infinite conductivity fracture and surface area of fracture have similar value of skin factor (figure 31).
5. Different fracture orientations intersecting vertical and horizontal wells do not impact the linear flow to the induced fracture with high or infinite conductivity model (figure 29, 30, and 33).
6. The pressure and derivative have similar behavior in injection and fall-off phases except at the late time of both periods.
7. Compound formation linear flow is exhibited in multi transverse induced fractures with adjacent distances in the horizontal well (figure 34).

4.2. Interference Tests

From previous scenarios, it is hard to perceive a unique response in the pressure derivative that distinguishes single transverse and longitudinal induced fractures by using a single-well testing method. Simulation of interference test are conducted to observe the differences in pressure responses of the observation well for two induced fracture orientations, parallel and perpendicular, which intercept the injection (active) well.

4.2.1. Comparison between Numerical and Analytical Simulations in Interference Tests (Non Fractured Well Cases)

The similar workflow with single-well test scenarios had been conducted where a starting point is comparison between results from analytical models and numerical simulations in base case.

Figure 35 displays the bottom-hole pressure profile in an observation well for case 7 and case 8. Interestingly, after the end of injection periods, the pressure keep continues to build up until the end of fall-off period. Low flow capacity (permeability) in the grid

block causes pressure to slow perturbations and responses in the observation well. Because of that reason, only injection phases are appropriate for interpretation of pressure transients in this interference tests study.

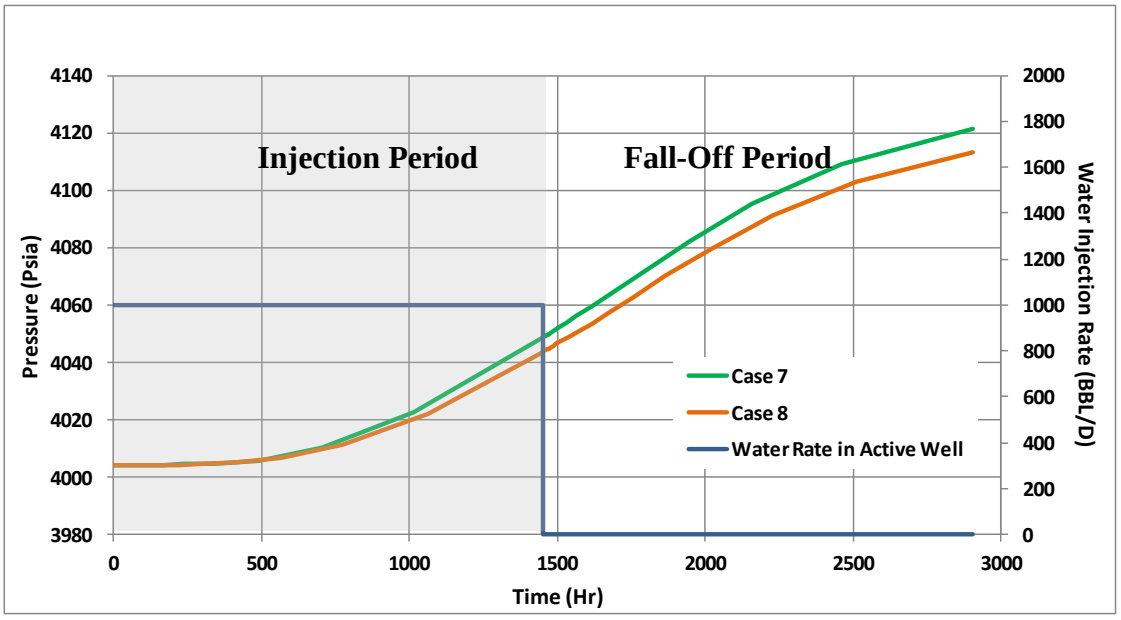

Figure 35: Pressure profiles in an observation well for vertical and horizontal injection wells.

As shown in figure 36, low permeability grid causes pressure transients to reach the observation well later at around 180 hour. It also leads to small changes in pressure buildup where the value is smaller than derivative responses during injection phases.

The analytical line source method shows a good match with case 7 (vertical well) as well as case 8 (horizontal well). It demonstrates not only comparable well and reservoir parameters had been achieved but also the grid size effect in the numerical simulation can be neglected. Also identical outcome for case 7 and 8 concludes that the geometry of injection well did not affect the response in the observation well.

It is then important to note that those summaries might not valid for some reservoir types, i.e. high permeability reservoir. Moreover, analytical study by Uraiet *et al.* (1977) pointed out that the distance between fractured active-observation wells affects the response in the observation well. Due to time limitation, this study did not consider the effect of the injection (active)-observation well distance.

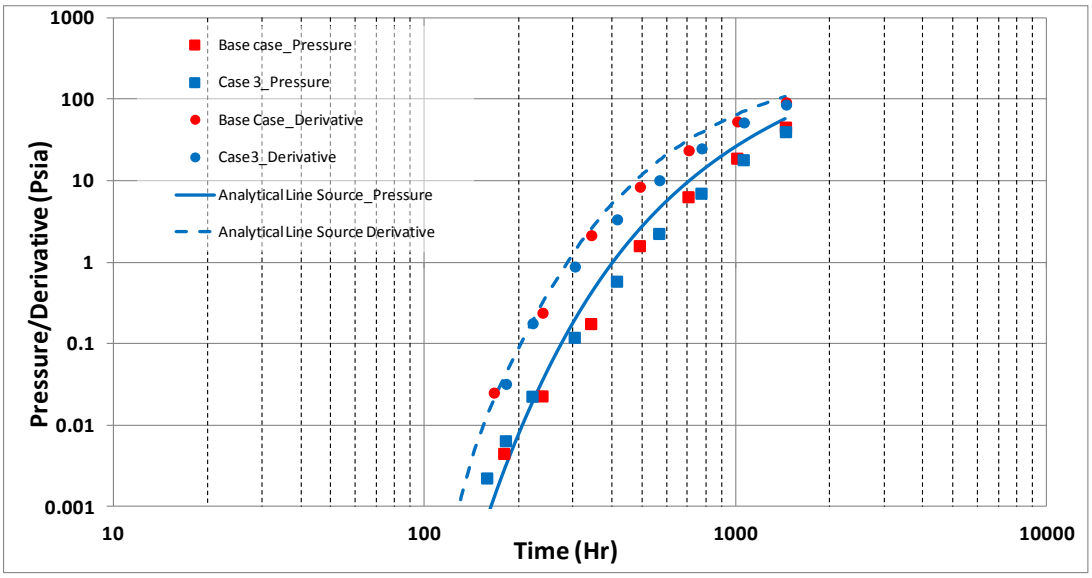

Figure 36: Pressures and derivatives of an observation well for vertical and horizontal injection (active) wells

4.2.2. Comparison between Longitudinal Induced Fracture and Transverse Induced Fracture in Interference Test.

Line Graphs in picture 37 represent the simulated pressure and derivative of fractured horizontal well compare with analytical line source model. Pressure and derivative curves, which were observed between longitudinal induced fracture (Case 9) and transverse induced fracture (case 10), have different slopes and there is a time shift between both cases. Consequently, case 10 will respond early but case 9 will respond lately compare to analytical solutions. In addition, there is no unique pressure derivative is exhibited between both cases.

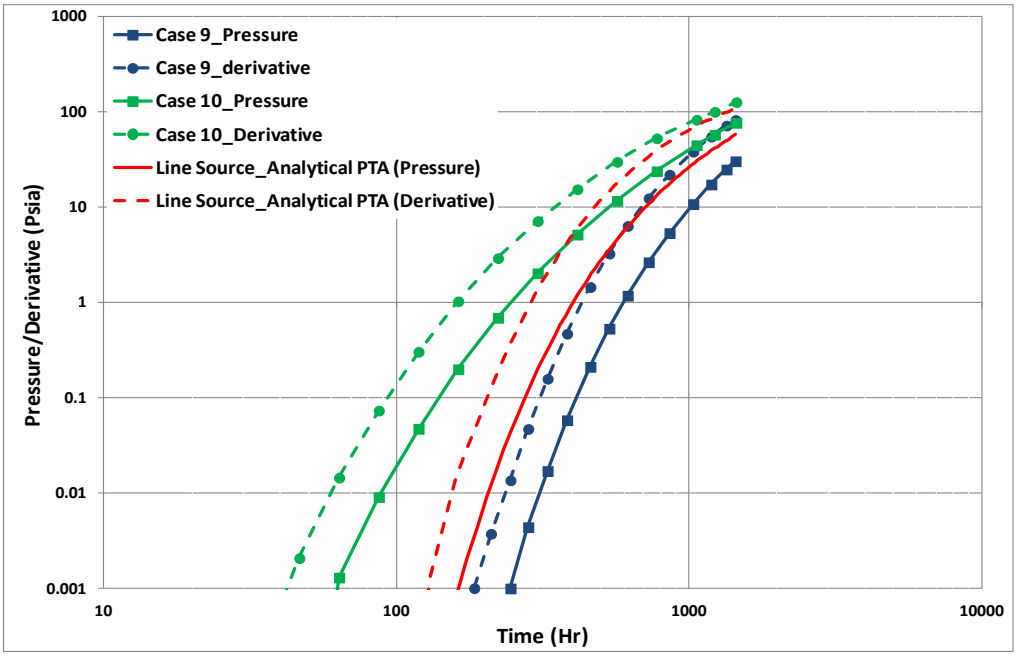

Figure 37: Pressures and derivatives in an observation well for fractured horizontal well cases

Figure 38 and figure 39 are essentially a visualization of phenomena explained by figure 37. From here, it is understood that the pressure is likely to flow within a fracture in the beginning and continue to travel toward formation afterwards. A induced transverse fracture creates a good pathway for the pressure to reach the observation well faster. Meanwhile in a longitudinal induced fracture, pressures would firstly fill the fracture in Y and Z direction (figure 39) causing a delay in reaching the observation well compared to case without fracture (case 8). From this analysis it can be summarized that induced fracture orientation intercepting an injection well affects the pressure distribution in the model thus will affects the time response in the observation well.

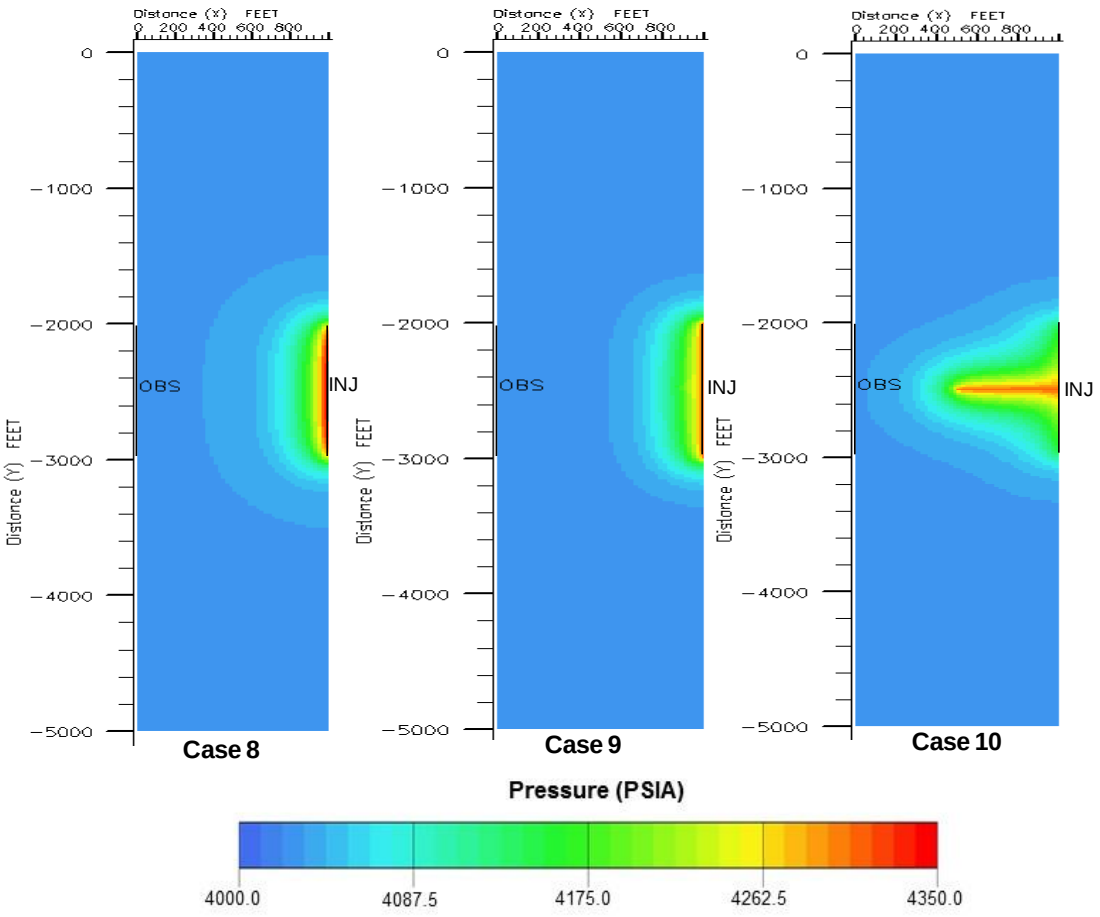

Figure 38: Impact of fracture orientation on the pressure distribution (at 200 hour)

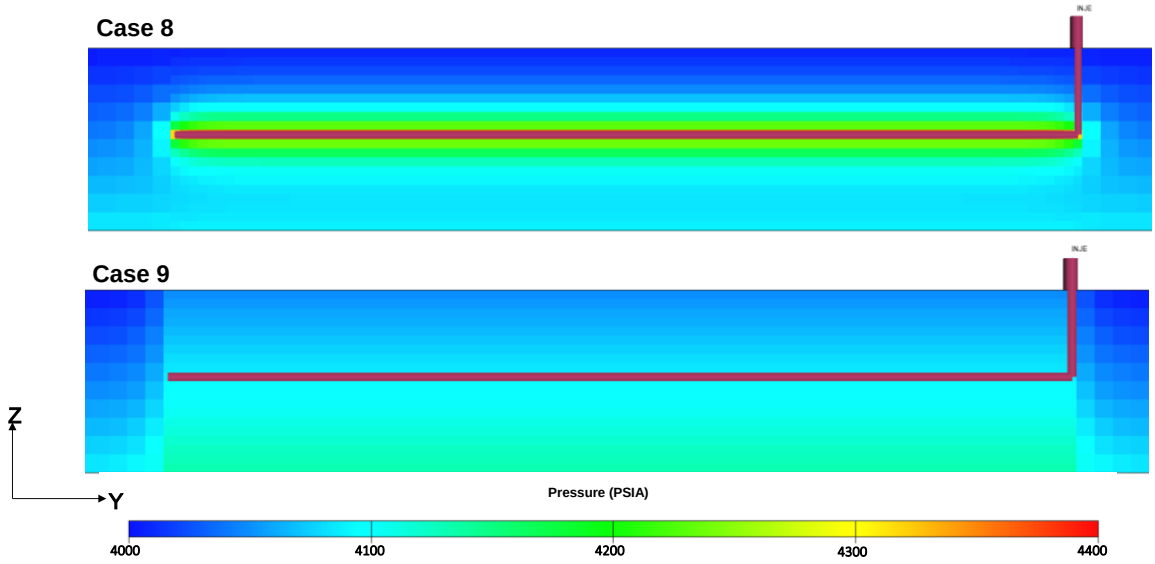

Figure 39: Impact of paralel fracture on the pressure distribution around an injection well (at 9 hour)

4.2.3. Impact of Pressure Dependent Fracture Permeability

By introducing a pressure dependent fracture permeability or $k_f(p)$, it can simulate that fracture is hydraulically induced from the injection (active) well and later observe the impact on the pressure transient in interference tests (please see section 3.4.2). Figure 40 and 41 describe the comparison between pressure and derivative of an observation well for $k_f(p)$ cases and constant fracture conductivity cases.

In longitudinal hydraulic induced fracture case, there is no effect to pressure transient responses of the observation well with the addition of $k_f(p)$. However, $k_f(p)$ has an impact in transverse hydraulic induced fracture (case 12) in which pressure transient responses of the observation well is delayed compared to case 10 (constant fracture conductivity).

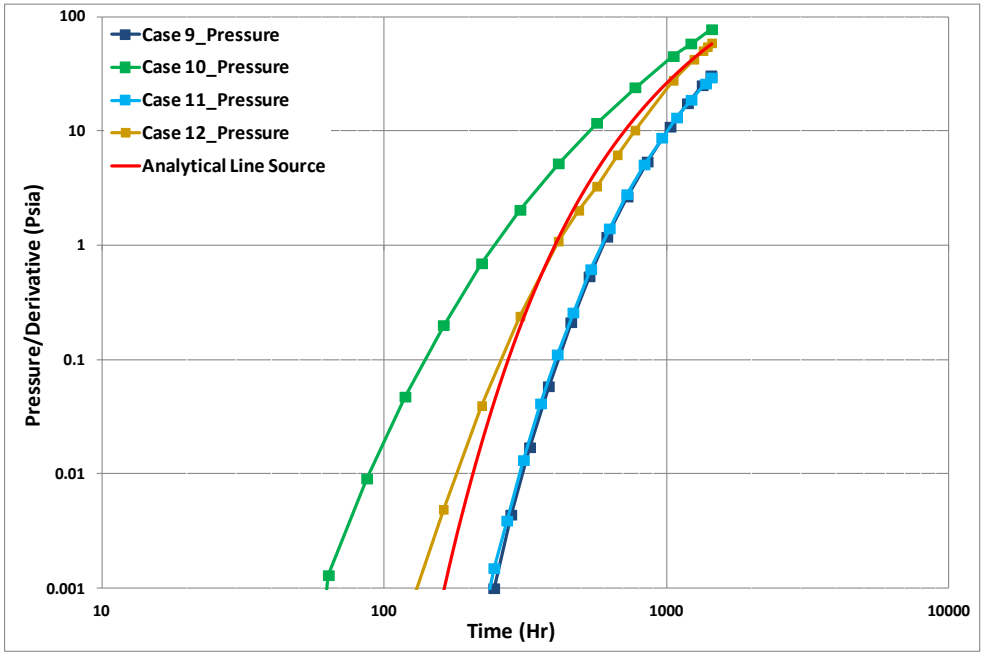

Figure 40: Pressure in an observation well for all induced fracture cases

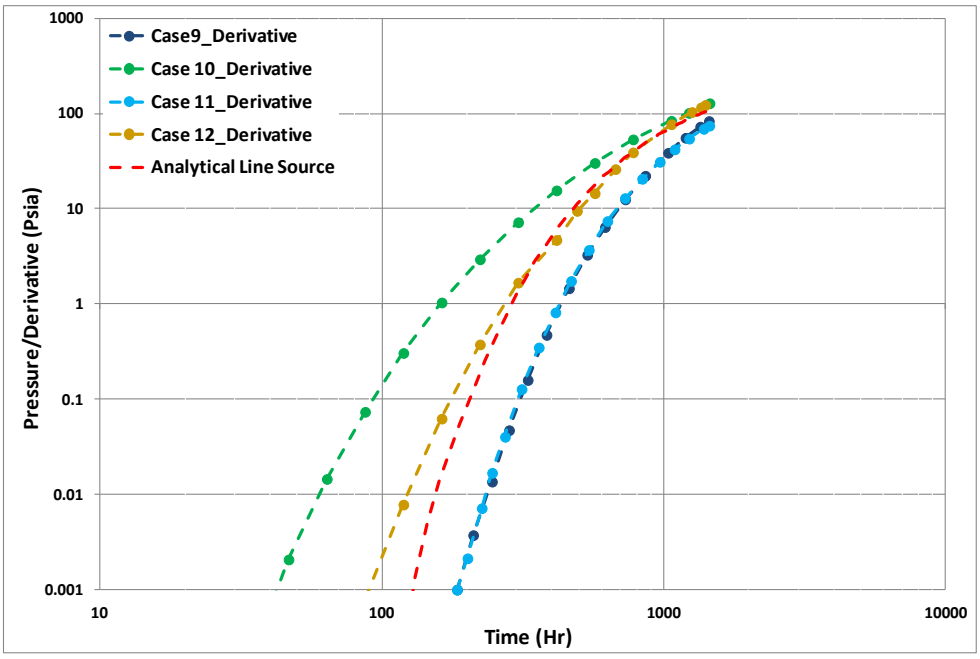

Figure 41: Pressure derivatives in an observation well for all induced fracture cases

As shown in figure 42, pressure perturbations in case 9 and case 11 have both similar behaviors (at 200 hour). In case 11, however, the pressure is initially spread throughout the horizontal well before propagate following the growth of perpendicular (transverse) induced fracture.

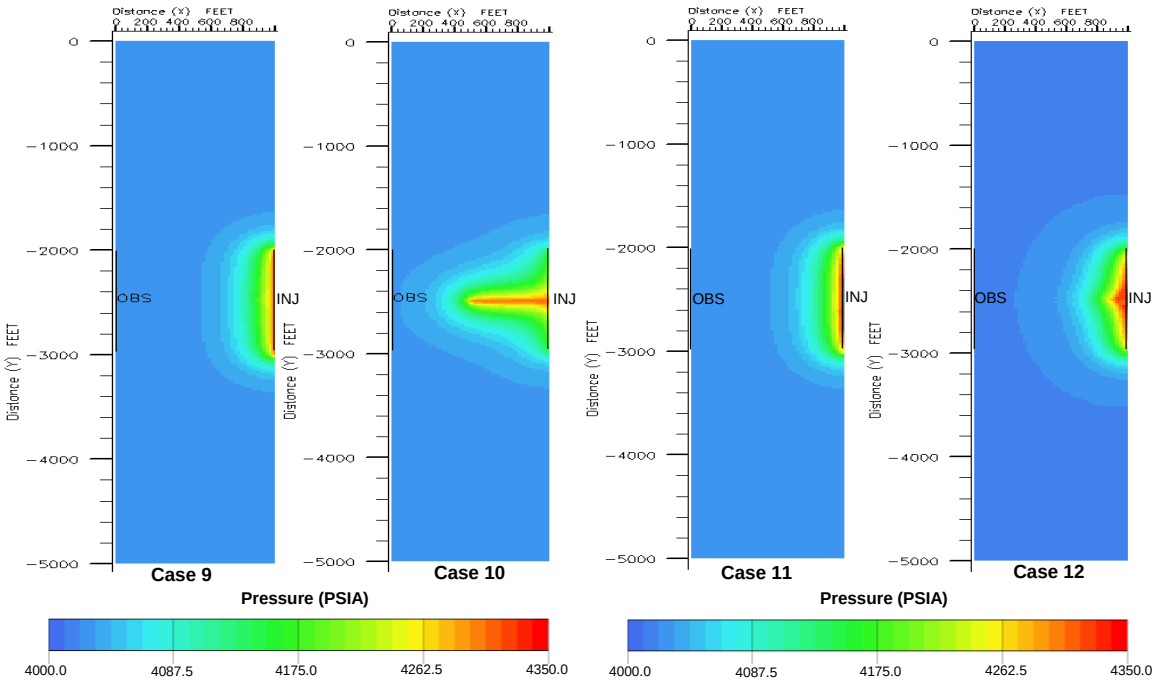

Figure 42: Impact of fracture orientation and $k_f(p)$ on the pressure distribution (at 200 hour)

In addition, if $k_f(p)$ is applied to transverse hydraulic induced fracture (case 12), the pressure and derivative will respond closely to solution from analytical line source. After 300 hour, the curve (case 12) shows a good match to line source analytical curve (figure 40 and 41).

4.2.4. Comparison to Analytical Well Tests Study

From the simulation of interference test study, pressure transients in the observation well show distinct outcomes in the response time for two cases of induced fracture orientation (parallel and perpendicular). So to confirm the result from this study, the analytical model from another study is presented and compared.

Meehan *et al*. (1989) reported that semi-analytical calculations in the interference test for both the observation and active well intercepted by finite conductivity hydraulic fractures. Their model showed that the orientation of fractures represented by fracture azimuth can be determined however the value of fracture length and fracture conductivity for each fracture cannot be determined uniquely from the interference test and should be analyzed independently.

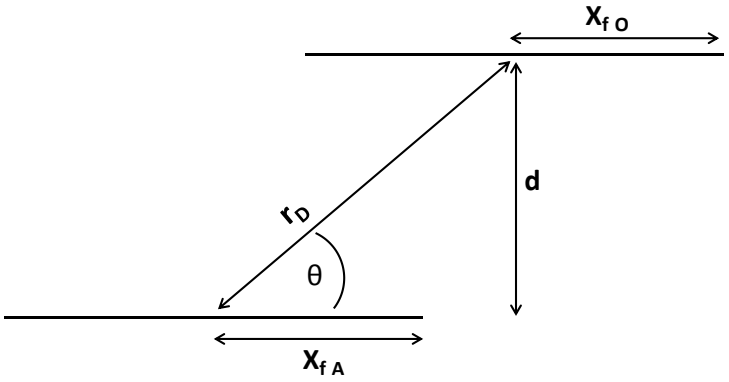

Figure 43: Illustration for fractured active-observation wells (adapted from Meehan *et al*. 1989)

Meehan *et al*. (1989) plotted the pressure and derivative response in the observation well for different fracture azimuth of 15 degrees until 90 degrees compare with analytical line source. They concluded that as the angle of azimuth increase the pressure will respond lately compared to 15 degrees of azimuth. They also concluded that the pressure responses from the active well are not sensitive to the observation well for $r_D \geq 2$.

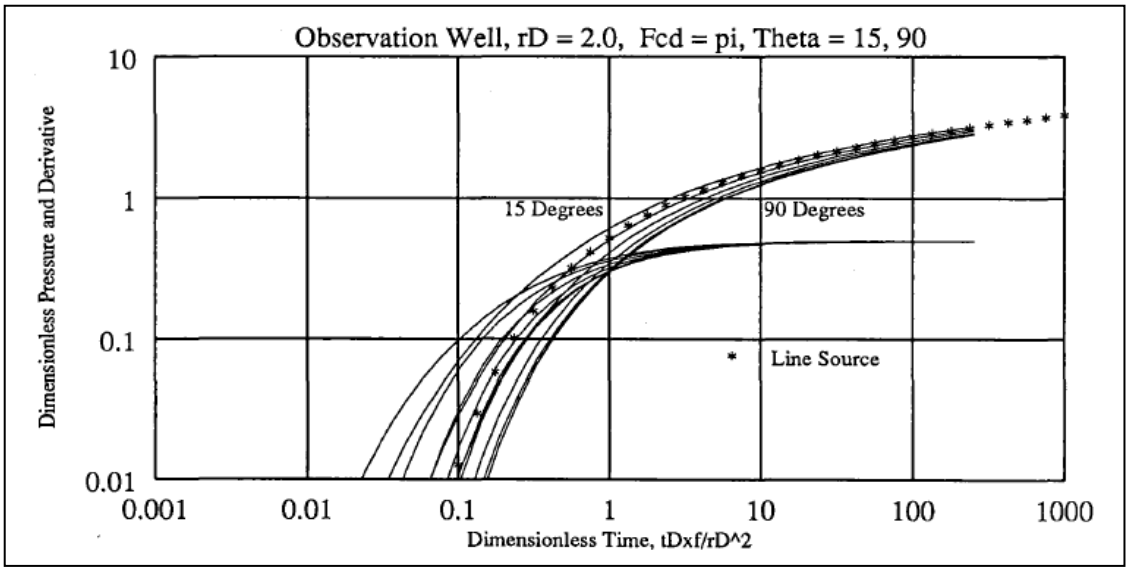

Figure 44: The pressure and derivative in the observation well for r_D = 2 (adapted from Meehan *et al.* 1989)

In conclusion, the pressure and derivative response achieved from author's numerical study (figure 37) shows similar behavior with the analysis from a reference (figure 44). Longitudinal induced fracture characterized by Azimuth 90 degrees in reference's result shows late response compared to transverse induced fracture in respect to azimuth 0 degrees.

4.2.5. Conclusions of Interference Test Study

The outcomes and analysis in this study show how numerical simulations and analytical models of well interference tests become a valuable tool that enables us to improve our understanding of induced fracture performance. Even though no unique derivative has been observed for pressure transients in the observation well, the time when pressure perturbation reaches the well provides good information of induced fracture direction.

Based on the numerical study for interference test following conclusions are presented:

1. In non-fracture case pressure transient responses of the observation well are independent to injection (active) well geometry (vertical or horizontal) if the horizontal well is not oriented towards the observation well.
2. Different fracture orientations have an impact on pressure distribution in the numerical simulation that will affect the time response on the observation well.
3. Longitudinal induced fracture intersecting the injection well causes a delay in response time of the observation well while transverse induced fracture intersecting the injection well leads to earlier arrival of pressure transient reach to the observation well (figure 37 and 38).

4. Delay of pressure transient responses on the observation well have been observed when $k_f(p)$ is introduced in transverse hydraulic induced fracture yet in longitudinal hydraulic induced fracture there is no effect of $k_f(p)$ to the response of the observation well (figure 40, 41, and 42).

5. Conclusions

This study examined different fluid flow regimes near wellbore and between wells governed by induced fractures and wells of different geometries using series of well test simulations with following analysis of resulted pressure responses. Two types of well tests, single-well tests and well interference tests were simulated with two fracture orientations (parallel and perpendicular to the well) and two well geometries (vertical and horizontal). For most of the cases, it was possible to generate identical responses with numerical and analytical simulations, that confirmed capabilities of analytical models in interpreting responses from many cases with complicated well and fracture geometries.

Main conclusions drawn from this study are as follows:

1. Although numerical simulation has more capabilities in simulating complicated well and fracture geometries and 3D effects, analytical models are also capable of reproducing many cases studied in the work.
2. When performing single-well tests of vertical and horizontal wells, different fracture orientations do not give an effect to the pressure derivative behavior in the case where the fracture has high or infinite conductivity. Only linear flow is exhibited in all single fracture cases with various geometries and orientations in this study.
3. In the simulation of well interference tests, different fracture orientations intersecting an active well have an impact on pressure distribution of simulated model that will affect the time response on the observation well. Accordingly, the time durations for designing well interference tests become important when determining the orientation of fracture.

The results and conclusions of this thesis may be implemented in the practical field application. A fractured horizontal well case is considered as a good example of how interpretation of simulated pressure responses may be used for designing actual well tests in order to understand performance of induced fractures. An interference test may be suggested to get some knowledge about induced fracture orientation, where an injection well connected by induced fracture may act as an active well and one of the nearby production wells may act as an observation well.

The interpretation of simulated pressure transient on the observation well showed that there is a time shift between responses from the parallel induced fracture and the perpendicular induced fracture (figure 37). The longest time of pressure response reached an observation well indicates the parallel induced fracture and may be used as the reference for the duration of the actual well test at which should cover all possibilities of induced fracture orientations. In this case injection phase may be the main part for the interpretation (see section 4.2.1 for explanation).

By plotting and comparing the actual pressure responses with synthetic pressure responses of parallel and perpendicular fracture, the understanding of actual orientation of induced fracture may be improved. Hence, this interpretation confirms the capability of the numerical simulation to suggest a well test design.

References

Bourdet, D., 2002. *Well Test Analysis : The Use of Advanced Interpretation Models.* Paris: Elsevier.

Bourdet, D., Whittle, T. M., Douglas, A. A. & Pirard, Y. M., 1983. A New Set of Type Curves Simplifies Well Test Analysis. *World Oil, May, 95-106. Gulf Publishing Co., Houston.*

Chen, C. C. & Raghavan, R., 1997. A Multiply-Fractured Horizontal Well in a Rectangular Drainage Region. *SPE paper 37072, International Conference on Horizontal Well Technology in Calgary,Canada.*

Cherifi, M., Tiab, D. & Escobar, F. H., 2002. Determination of Fracture Orientation by Multi-Well Interference Testing. *SPE paper 77949, SPE Asia Pacific Oil and Gas Conference and Exhibition, Melbourne, Australia..*

Cinco-ley, H. & Samaniego, F., 1977. Determination of The orientation of A Finite Conductivity Vertical Fracture By Transient Pressure Analysis. *SPE paper 6750-MS, 52nd Annual Fall Technical Conference and Exhibition of The SPE AIME, Denver, Colorado.*

Cinco-Ley, H. & Samaniego, F., 1981. Transient Pressure Analysis for Fractured Wells. *SPE paper 7490, SPE 53rd Annual Technical Conference and Exhibition, Houston.*

E.Fjaer, R. H., P.Horsrud, A. R. & Risnes, R., 2008. *Petroleum Related Rock Mechanics 2nd Edition.* s.l.:Elsevier.

Earlogher, R. C. J., 1977. *Advances in Well Test Analysis.* Dallas: Society of Petroleum Engineers of AIME.

Egya, D. et al., 2016. Assessing the Validity and Limitations of Dual-Porosity Models Using Geological Well Testing for Fractured Formations. *78th EAGE Conference & Exhibition, Vienna, Austria.*

Elkins, L. F. & Skov, A. M., 1960. Determination of Fracture Orientation from Pressure Interference. *SPE AIME, 35 th Annual Fall Meeting of SPE, Denver.*

Gringarten, A. C., Ramey, H. J. & Raghavan, R., 1974. Unsteady-State Pressure Distribution Created by a Well with a Single Infinite Conductivity Fracture. *Society of Petroleum Engineer Journal, August,* pp. 413-426.

Hegre, T. M., 1996. Hydraulically Fractured Horizontal Well Simulation. *SPE paper 35506, European 3-D Reservoir Modeling Conference, Stavanger, Norway.*

Horne, R. N., 1995. *Modern Well Test Analysis.* Palo Alto, California: Petroway, Inc.

Husted, B., Zwarts, D., Masfry, R. & Van Den Hoek, P. J., 2006. Induced Fracturing in Reservoir Simulations: Application of a New Coupled Simulator to Waterflooding Field Examples. *SPE paper 102467, SPE Annual Technical Conference and Exhibition, San Antonio, Texas, U.S.A.*

Jargon, J. R., 1976. Effet of Wellbore Storage and Wellbore Damage at the Active Well on Interference Test Analysis. *Journal Petroleum Technology., Aug,* pp. 851-858.

Kamal, M. M., Pan, Y., Landa, J. L. & Thomas, O. O., 2005. Numerical Well Testing-A Method To Use Transient Testing Results in Reservoir Simulation. *SPE paper 95905, SPE Annual Technical Conference and Exhibition held in Dallas, Texas, U.S.A.*

Lacy, L. L., 1987. Comparison of Hydraulic-Fracture Orientation Techniques. *SPE Formation Evaluation.*

Lafond, K. B., Pederson, L. M. & Christiansen, L. B., 2010. FAST Optimization of Line Drive Water Injection. *SPE 130471,* p. 16.

Larsen, L., 1998. Productivities of Fractured and Nonfractured Deviated Wells in Commingle Layered Reservoirs. *SPE paper 38912, SPE Annual Technical Conference and Exhibition, San Antonio, Texas.*

Larsen, L., 2010. *Well Testing - Analysis of Pressure Transient Data.* Stavanger: University of Stavanger.

Larsen, L. & Hegre, T. M., 1994 a. Pressure Transient Analysis of Multifractured Horizontal Wells. *SPE paper 28389, SPE 69th Annual Technical Conference and Exhibition, New Orleans, LA, USA.*

Larsen, L. & Hegre, T. M., 1994 b. Productivity of Multifractured Horizontal Wells. *SPE paper 28845, European Petroleum Conference, London, U.K.*

Ma, Q. & Tiab, D., 1995. Interference Test Analysis in Naturally Fractured Reservoirs. *SPE paper 29514, Production Operations Symposium, Oklahoma City, OK, U.S.A.*

Matthews, C. S. & Russel, D. G., 1967. *Pressure Build-up and Flow Tests in Wells.* s.l.:Monograph Series no 1, Society of Petroleum Engineers of AIME..

Meehan., D. e. a., 1989. Interference Testing of Finite Conductivity Hydraulically Fractured Wells. *SPE 19784,* p. 9.

Morton, K. L., Nugueira, P. d. B., Booth, R. S. & Kuchuk, F. J., 2012. Integrated Interpretation for Pressure Transient Tests in Discretely Fractured Reservois. *SPE peper 154531, EAGE Annual Conference & Exhibition incorporating SPE Europec held in Copenhagen, Denmark.*

Mousli, N. A., Raghavan, R., Cinco-Ley, H. & Samaniego, F., 1982. The Influence of Vertical Fractures Intercepting Active and Observation Wells on Interference Tests. *SPE paper 9346, Society of Petroleum Engineers Journal, SPE Annual Technical Conference and Exhibition, Dallas.*

Pan, Y. et al., 2013. Integration of Pressure Transient Data in Modeling Tengiz Field, Kazakhstan-A New Way to Characterize Fractured Reservoirs. *SPE paper 165322, SPE Western Region & AAPG Pacific Section Meeting, 2013 Joint Technical Conference, Monterey, California, U.S.A.*

Pierce, A. E., Vela, S. & Koonce, K. T., 1975. Determination of the Compass Orientation and Length of Hydraulic Fractures by Pulse Testing. *SPE-AIME, the SPE-AIME 49th Annual Fall Meeting, Houston.*

Raghavan, R. & Chin, L. Y., 2004. Productivity Changes in Reservoir with Stress-Dependent Permeability. *SPE paper 88870, SPE Annual Technical Conference and Exhibition, San Antonio, Texas.*

Rod, M. H. & JØrgensen, O., 2005. Injection Fracturing in a Densely Spaced Line Drive Waterflood-The Hafdan Example. *SPE paper 94049, SPE Europec/EAGE Annual Conference, Madrid, Spain.*

Shchipanov, A. A., Berenblyum, R. A. & Kollbotn, L., 2014. Pressure Transient Analysis as an Element of Permanent Reservoir Monitoring. *SPE paper170740-MS, the SPE Annual Technical Conference and Exhibition, Amsterdam, The Netherlands.*

Soliman, M. Y., Azari, M., Hunt, J. L. & Chen, C. C., 1996. Design and Analysis of Fractured Horizontal Wells in Gas Reservoirs. *SPE paper 35343, The International Petroleum Conference and Exhibition of Mexico, Villahermosa, Mexico.*

Soliman, M. Y., Hunt, J. L. & EL Rabaa, A. M., 1990. Fracturing Aspects of Horizontal Wells. *SPE paper 18542, SPE Eastern Regional Meeting, Charleston, WV.*

Spencer, T. W. & Chi, H. C., 1989. Seismic Determination of Fracture Orientation. *SEG.*

Theis, C. V., 1935. The Relation Between the Lowering of the Piezometric Surface and the Rate and Duration of Discharge of a Well Using Ground-Water Storage. *Trans. AGU 519-524.*

Tiab, D. & Abobise, E. O., 1989. Determination Fracture Orientation From Pulse Testing. *SPE Formation Evaluation.*

Tiab, D. & Kumar, A., 1980. Detection and Location of Two Parallel Sealing Faults Around a Well. *Journal of Petroleum Technology,* pp. 1701-1708.

Uraiet, A., Raghavan, R. & Thomas, G. W., 1977. Determination of the Orientation of a Vertical Fracture by Interference Tests. *SPE-AIME*.

Wei, L. et al., 1998. Discriminating Fracture Patterns in Fractured Reservoirs by Pressure Transient Tests. *SPE paper 49233, The SPE Annual Technical Conference and Exhibition, New Orlean, Louisiana.*

Nomenclature

B Formation volume factor, $RB/STB\ or\ Rm^3/Sm^3$

B_w Water Formation volume factor, $RB/STB\ or\ Rm^3/Sm^3$

C_t Total compressibility, $psia^{-1}\ or\ bar^{-1}$

e Exponential (2.7182…)

Ei Exponential integral

h Reservoir thickness, $ft\ or\ m$

h_f Fracture thickness, md

k Permeability, md

k_f Fracture permeability, md

$k_f(p)$ Pressure dependent fracture permeability, md

k_i Initial permeability, md

k_x Permeability in x direction, md

k_y Permeability in y direction, md

k_z Permeability in z direction, md

m Straight line slope, $psia/cycle$

P Pressure, $psia\ or\ bar$

P_D Dimensionless pressure

Pi Initial pressure, $psia\ or\ bar$

q Flow rate, $Sm^3/day\ or\ STB/day$

r Radial distance to the well, $ft\ or\ m$

r_D Dimensionless radius

r_w Well radius, ft

s Skin factor, dimensionless

t Time, hr

t_D Dimensionless time

t_p Production time, hr

x_e Model length, ft

x_f Fracture half length, ft

x_i Distance between active well and observation well, ft

y_e Model length, ft

y_f Distance to neighboring fractures, ft

y_{fD} Dimensionless of fracture half length

y_p Permeability modulus parameter, $psia^{-1}$

z_w Distance from a horizontal well to the lower boundary, ft

$\Delta P'$ Pressure derivative, $psia\ or\ bar$

Δt Elapsed time or build-up time, hr

ΔP Pressure change, $psia\ or\ bar$

μ Viscosity, cp

μ_w Water viscosity, cp

$\boldsymbol{\phi}$ Porosity, $fraction$

Abbreviations

BHP	Bottom Hole Pressure, *psia or bars*
INJ	Injection well
LGR	Local Grid Refinement
OBS	Observation well
PI	Productivity Index
PSS	Pseudo Steady State
PTA	Pressure Transient Analysis

Appendix

Appendix A – Eclipse models

The Eclipse code below was used to simulate interference tests and single-well tests of longitudinal induced fracture intersecting a horizontal well. Some modifications were made such as implementing pressure dependent fracture permeability.

```
--By Anggi Putra Yanse

RUNSPEC    ======================
TITLE
  SIMULATION OF INTEFERENCE TEST FOR INDUCED FRACTURE

DIMENS

50 250 10/

OIL
WATER
FIELD

WELLDIMS
500 500 2 2 /

FRICTION
2 2 /

NOECHO

START

1 'FEB' 2015 /

NSTACK
25 /

LGR
5 50000 10 6 6 /

UNIFOUT

UNIFIN

GRID       ======================

INIT

NOECHO
```

```
DX
125000*20/

DY
125000*20/

DZ
125000*20 /

PERMX
125000*1/

PERMY
125000*1/

PERMZ
125000*1/

PORO
125000*0.3/

TOPS
12500*7000  12500*7020  12500*7040  12500*7060  12500*7080  12500*7100  12500*7120
12500*7140 12500*7160 12500*7180 /

CARFIN
--ACTIVE LOCAL GRID REFINEMENT
'LGR1' 50 50 101 150 1 10 5 100 20 10 /

HXFIN
-- ACTIVE HXFIN AND REFINE TO IMPLEMENT INDUCED FRACTURE
10.2 5.2 2.4 1.2 1/

REFINE
'LGR1' /
EQUALS
'PERMY' 250000 5 5 1 100 1 20 /
'PERMZ' 250000 5 5 1 100 1 20 /
/

ENDFIN

CARFIN

'LGR2' 1 1 101 150 1 10 5 100 20 10 /

HXFIN
1 1.2 2.4 5.2 10.2/

REFINE
'LGR2' /
```

```
EQUALS
'PERMY' 250000 1 1 1 100 1 20 /
'PERMZ' 250000 1 1 1 100 1 20 /
/

ENDFIN

AMALGAM
'LGR1' 'LGR2'/
/

RPTGRID
/

PROPS   ======================
NOECHO

ROCK
7000  6.0E-6   /

SWOF
 0.2 0 1 0
 0.3 0.03 0.69 0
 0.4 0.11 0.44 0
 0.5 0.25 0.25 0
 0.6 0.44 0.11 0
 0.7 0.69 0.03 0
 0.8 1 0 0
/

PVTW
7000 1 4.0E-6 1 0/

PVCDO
7000 1 0 0.5 0/

DENSITY
52  64  0.05 /


SOLUTION   ============================

EQUIL
7000 4000 7000 /

RPTSOL
'RESTART=2' /

RPTRST

'BASIC=6' ROCKC /
```

```
SUMMARY     ============================

NOECHO

EXCEL

DATE

FWPR

FOPR

FWCT

WBHP
'INJ' 'OBS'/

FWIR

SCHEDULE    ============================

RPTSCHED
'RESTART=2' /

MESSAGES
 9*  10000   2*  /

WELSPECL
--INJ REFERS TO INJECTION WELL WHILE OBS REFERS TO OBSERVATION WELL
'INJ' 'G' 'LGR1' 5 1 1* 'WATER'/
'OBS' 'G' 'LGR2' 1 1 1* 'WATER'/
/
-- ACTIVE COMPDATL AND WFRICTNL TO IMPLEMENT HORIZONTAL WELL

COMPDATL
'INJ'     'LGR1'   5        1        10       10       'OPEN'  2*       0.5      /
'INJ'     'LGR1'   5        2        10       10       'OPEN'  2*       0.5      /
'INJ'     'LGR1'   5        3        10       10       'OPEN'  2*       0.5      /
'INJ'     'LGR1'   5        4        10       10       'OPEN'  2*       0.5      /
'INJ'     'LGR1'   5        5        10       10       'OPEN'  2*       0.5      /
'INJ'     'LGR1'   5        6        10       10       'OPEN'  2*       0.5      /
'INJ'     'LGR1'   5        7        10       10       'OPEN'  2*       0.5      /
'INJ'     'LGR1'   5        8        10       10       'OPEN'  2*       0.5      /
'INJ'     'LGR1'   5        9        10       10       'OPEN'  2*       0.5      /
'INJ'     'LGR1'   5        10       10       10       'OPEN'  2*       0.5      /
'INJ'     'LGR1'   5        11       10       10       'OPEN'  2*       0.5      /
'INJ'     'LGR1'   5        12       10       10       'OPEN'  2*       0.5      /
'INJ'     'LGR1'   5        13       10       10       'OPEN'  2*       0.5      /
'INJ'     'LGR1'   5        14       10       10       'OPEN'  2*       0.5      /
```

```
'INJ'   'LGR1'  5   15   10   10   'OPEN'  2*   0.5   /
'INJ'   'LGR1'  5   16   10   10   'OPEN'  2*   0.5   /
'INJ'   'LGR1'  5   17   10   10   'OPEN'  2*   0.5   /
'INJ'   'LGR1'  5   18   10   10   'OPEN'  2*   0.5   /
'INJ'   'LGR1'  5   19   10   10   'OPEN'  2*   0.5   /
'INJ'   'LGR1'  5   20   10   10   'OPEN'  2*   0.5   /
'INJ'   'LGR1'  5   21   10   10   'OPEN'  2*   0.5   /
'INJ'   'LGR1'  5   22   10   10   'OPEN'  2*   0.5   /
'INJ'   'LGR1'  5   23   10   10   'OPEN'  2*   0.5   /
'INJ'   'LGR1'  5   24   10   10   'OPEN'  2*   0.5   /
'INJ'   'LGR1'  5   25   10   10   'OPEN'  2*   0.5   /
'INJ'   'LGR1'  5   26   10   10   'OPEN'  2*   0.5   /
'INJ'   'LGR1'  5   27   10   10   'OPEN'  2*   0.5   /
'INJ'   'LGR1'  5   28   10   10   'OPEN'  2*   0.5   /
'INJ'   'LGR1'  5   29   10   10   'OPEN'  2*   0.5   /
'INJ'   'LGR1'  5   30   10   10   'OPEN'  2*   0.5   /
'INJ'   'LGR1'  5   31   10   10   'OPEN'  2*   0.5   /
'INJ'   'LGR1'  5   32   10   10   'OPEN'  2*   0.5   /
'INJ'   'LGR1'  5   33   10   10   'OPEN'  2*   0.5   /
'INJ'   'LGR1'  5   34   10   10   'OPEN'  2*   0.5   /
'INJ'   'LGR1'  5   35   10   10   'OPEN'  2*   0.5   /
'INJ'   'LGR1'  5   36   10   10   'OPEN'  2*   0.5   /
'INJ'   'LGR1'  5   37   10   10   'OPEN'  2*   0.5   /
'INJ'   'LGR1'  5   38   10   10   'OPEN'  2*   0.5   /
'INJ'   'LGR1'  5   39   10   10   'OPEN'  2*   0.5   /
'INJ'   'LGR1'  5   40   10   10   'OPEN'  2*   0.5   /
'INJ'   'LGR1'  5   41   10   10   'OPEN'  2*   0.5   /
'INJ'   'LGR1'  5   42   10   10   'OPEN'  2*   0.5   /
'INJ'   'LGR1'  5   43   10   10   'OPEN'  2*   0.5   /
'INJ'   'LGR1'  5   44   10   10   'OPEN'  2*   0.5   /
'INJ'   'LGR1'  5   45   10   10   'OPEN'  2*   0.5   /
'INJ'   'LGR1'  5   46   10   10   'OPEN'  2*   0.5   /
'INJ'   'LGR1'  5   47   10   10   'OPEN'  2*   0.5   /
'INJ'   'LGR1'  5   48   10   10   'OPEN'  2*   0.5   /
'INJ'   'LGR1'  5   49   10   10   'OPEN'  2*   0.5   /
'INJ'   'LGR1'  5   50   10   10   'OPEN'  2*   0.5   /
'INJ'   'LGR1'  5   51   10   10   'OPEN'  2*   0.5   /
'INJ'   'LGR1'  5   52   10   10   'OPEN'  2*   0.5   /
'INJ'   'LGR1'  5   53   10   10   'OPEN'  2*   0.5   /
'INJ'   'LGR1'  5   54   10   10   'OPEN'  2*   0.5   /
'INJ'   'LGR1'  5   55   10   10   'OPEN'  2*   0.5   /
'INJ'   'LGR1'  5   56   10   10   'OPEN'  2*   0.5   /
'INJ'   'LGR1'  5   57   10   10   'OPEN'  2*   0.5   /
'INJ'   'LGR1'  5   58   10   10   'OPEN'  2*   0.5   /
'INJ'   'LGR1'  5   59   10   10   'OPEN'  2*   0.5   /
'INJ'   'LGR1'  5   60   10   10   'OPEN'  2*   0.5   /
'INJ'   'LGR1'  5   61   10   10   'OPEN'  2*   0.5   /
'INJ'   'LGR1'  5   62   10   10   'OPEN'  2*   0.5   /
'INJ'   'LGR1'  5   63   10   10   'OPEN'  2*   0.5   /
'INJ'   'LGR1'  5   64   10   10   'OPEN'  2*   0.5   /
'INJ'   'LGR1'  5   65   10   10   'OPEN'  2*   0.5   /
```

```
'INJ'  'LGR1'  5  66   10  10  'OPEN'  2*  0.5  /
'INJ'  'LGR1'  5  67   10  10  'OPEN'  2*  0.5  /
'INJ'  'LGR1'  5  68   10  10  'OPEN'  2*  0.5  /
'INJ'  'LGR1'  5  69   10  10  'OPEN'  2*  0.5  /
'INJ'  'LGR1'  5  70   10  10  'OPEN'  2*  0.5  /
'INJ'  'LGR1'  5  71   10  10  'OPEN'  2*  0.5  /
'INJ'  'LGR1'  5  72   10  10  'OPEN'  2*  0.5  /
'INJ'  'LGR1'  5  73   10  10  'OPEN'  2*  0.5  /
'INJ'  'LGR1'  5  74   10  10  'OPEN'  2*  0.5  /
'INJ'  'LGR1'  5  75   10  10  'OPEN'  2*  0.5  /
'INJ'  'LGR1'  5  76   10  10  'OPEN'  2*  0.5  /
'INJ'  'LGR1'  5  77   10  10  'OPEN'  2*  0.5  /
'INJ'  'LGR1'  5  78   10  10  'OPEN'  2*  0.5  /
'INJ'  'LGR1'  5  79   10  10  'OPEN'  2*  0.5  /
'INJ'  'LGR1'  5  80   10  10  'OPEN'  2*  0.5  /
'INJ'  'LGR1'  5  81   10  10  'OPEN'  2*  0.5  /
'INJ'  'LGR1'  5  82   10  10  'OPEN'  2*  0.5  /
'INJ'  'LGR1'  5  83   10  10  'OPEN'  2*  0.5  /
'INJ'  'LGR1'  5  84   10  10  'OPEN'  2*  0.5  /
'INJ'  'LGR1'  5  85   10  10  'OPEN'  2*  0.5  /
'INJ'  'LGR1'  5  86   10  10  'OPEN'  2*  0.5  /
'INJ'  'LGR1'  5  87   10  10  'OPEN'  2*  0.5  /
'INJ'  'LGR1'  5  88   10  10  'OPEN'  2*  0.5  /
'INJ'  'LGR1'  5  89   10  10  'OPEN'  2*  0.5  /
'INJ'  'LGR1'  5  90   10  10  'OPEN'  2*  0.5  /
'INJ'  'LGR1'  5  91   10  10  'OPEN'  2*  0.5  /
'INJ'  'LGR1'  5  92   10  10  'OPEN'  2*  0.5  /
'INJ'  'LGR1'  5  93   10  10  'OPEN'  2*  0.5  /
'INJ'  'LGR1'  5  94   10  10  'OPEN'  2*  0.5  /
'INJ'  'LGR1'  5  95   10  10  'OPEN'  2*  0.5  /
'INJ'  'LGR1'  5  96   10  10  'OPEN'  2*  0.5  /
'INJ'  'LGR1'  5  97   10  10  'OPEN'  2*  0.5  /
'INJ'  'LGR1'  5  98   10  10  'OPEN'  2*  0.5  /
'INJ'  'LGR1'  5  99   10  10  'OPEN'  2*  0.5  /
'INJ'  'LGR1'  5  100  10  10  'OPEN'  2*  0.5  /
'OBS'  'LGR2'  1  1    10  10  'OPEN'  2*  0.5  /
'OBS'  'LGR2'  1  2    10  10  'OPEN'  2*  0.5  /
'OBS'  'LGR2'  1  3    10  10  'OPEN'  2*  0.5  /
'OBS'  'LGR2'  1  4    10  10  'OPEN'  2*  0.5  /
'OBS'  'LGR2'  1  5    10  10  'OPEN'  2*  0.5  /
'OBS'  'LGR2'  1  6    10  10  'OPEN'  2*  0.5  /
'OBS'  'LGR2'  1  7    10  10  'OPEN'  2*  0.5  /
'OBS'  'LGR2'  1  8    10  10  'OPEN'  2*  0.5  /
'OBS'  'LGR2'  1  9    10  10  'OPEN'  2*  0.5  /
'OBS'  'LGR2'  1  10   10  10  'OPEN'  2*  0.5  /
'OBS'  'LGR2'  1  11   10  10  'OPEN'  2*  0.5  /
'OBS'  'LGR2'  1  12   10  10  'OPEN'  2*  0.5  /
'OBS'  'LGR2'  1  13   10  10  'OPEN'  2*  0.5  /
'OBS'  'LGR2'  1  14   10  10  'OPEN'  2*  0.5  /
'OBS'  'LGR2'  1  15   10  10  'OPEN'  2*  0.5  /
'OBS'  'LGR2'  1  16   10  10  'OPEN'  2*  0.5  /
```

```
'OBS'   'LGR2'  1       17      10      10      'OPEN'  2*      0.5     /
'OBS'   'LGR2'  1       18      10      10      'OPEN'  2*      0.5     /
'OBS'   'LGR2'  1       19      10      10      'OPEN'  2*      0.5     /
'OBS'   'LGR2'  1       20      10      10      'OPEN'  2*      0.5     /
'OBS'   'LGR2'  1       21      10      10      'OPEN'  2*      0.5     /
'OBS'   'LGR2'  1       22      10      10      'OPEN'  2*      0.5     /
'OBS'   'LGR2'  1       23      10      10      'OPEN'  2*      0.5     /
'OBS'   'LGR2'  1       24      10      10      'OPEN'  2*      0.5     /
'OBS'   'LGR2'  1       25      10      10      'OPEN'  2*      0.5     /
'OBS'   'LGR2'  1       26      10      10      'OPEN'  2*      0.5     /
'OBS'   'LGR2'  1       27      10      10      'OPEN'  2*      0.5     /
'OBS'   'LGR2'  1       28      10      10      'OPEN'  2*      0.5     /
'OBS'   'LGR2'  1       29      10      10      'OPEN'  2*      0.5     /
'OBS'   'LGR2'  1       30      10      10      'OPEN'  2*      0.5     /
'OBS'   'LGR2'  1       31      10      10      'OPEN'  2*      0.5     /
'OBS'   'LGR2'  1       32      10      10      'OPEN'  2*      0.5     /
'OBS'   'LGR2'  1       33      10      10      'OPEN'  2*      0.5     /
'OBS'   'LGR2'  1       34      10      10      'OPEN'  2*      0.5     /
'OBS'   'LGR2'  1       35      10      10      'OPEN'  2*      0.5     /
'OBS'   'LGR2'  1       36      10      10      'OPEN'  2*      0.5     /
'OBS'   'LGR2'  1       37      10      10      'OPEN'  2*      0.5     /
'OBS'   'LGR2'  1       38      10      10      'OPEN'  2*      0.5     /
'OBS'   'LGR2'  1       39      10      10      'OPEN'  2*      0.5     /
'OBS'   'LGR2'  1       40      10      10      'OPEN'  2*      0.5     /
'OBS'   'LGR2'  1       41      10      10      'OPEN'  2*      0.5     /
'OBS'   'LGR2'  1       42      10      10      'OPEN'  2*      0.5     /
'OBS'   'LGR2'  1       43      10      10      'OPEN'  2*      0.5     /
'OBS'   'LGR2'  1       44      10      10      'OPEN'  2*      0.5     /
'OBS'   'LGR2'  1       45      10      10      'OPEN'  2*      0.5     /
'OBS'   'LGR2'  1       46      10      10      'OPEN'  2*      0.5     /
'OBS'   'LGR2'  1       47      10      10      'OPEN'  2*      0.5     /
'OBS'   'LGR2'  1       48      10      10      'OPEN'  2*      0.5     /
'OBS'   'LGR2'  1       49      10      10      'OPEN'  2*      0.5     /
'OBS'   'LGR2'  1       50      10      10      'OPEN'  2*      0.5     /
'OBS'   'LGR2'  1       51      10      10      'OPEN'  2*      0.5     /
'OBS'   'LGR2'  1       52      10      10      'OPEN'  2*      0.5     /
'OBS'   'LGR2'  1       53      10      10      'OPEN'  2*      0.5     /
'OBS'   'LGR2'  1       54      10      10      'OPEN'  2*      0.5     /
'OBS'   'LGR2'  1       55      10      10      'OPEN'  2*      0.5     /
'OBS'   'LGR2'  1       56      10      10      'OPEN'  2*      0.5     /
'OBS'   'LGR2'  1       57      10      10      'OPEN'  2*      0.5     /
'OBS'   'LGR2'  1       58      10      10      'OPEN'  2*      0.5     /
'OBS'   'LGR2'  1       59      10      10      'OPEN'  2*      0.5     /
'OBS'   'LGR2'  1       60      10      10      'OPEN'  2*      0.5     /
'OBS'   'LGR2'  1       61      10      10      'OPEN'  2*      0.5     /
'OBS'   'LGR2'  1       62      10      10      'OPEN'  2*      0.5     /
'OBS'   'LGR2'  1       63      10      10      'OPEN'  2*      0.5     /
'OBS'   'LGR2'  1       64      10      10      'OPEN'  2*      0.5     /
'OBS'   'LGR2'  1       65      10      10      'OPEN'  2*      0.5     /
'OBS'   'LGR2'  1       66      10      10      'OPEN'  2*      0.5     /
'OBS'   'LGR2'  1       67      10      10      'OPEN'  2*      0.5     /
```

```
'OBS'   'LGR2'  1       68      10      10      'OPEN'  2*      0.5     /
'OBS'   'LGR2'  1       69      10      10      'OPEN'  2*      0.5     /
'OBS'   'LGR2'  1       70      10      10      'OPEN'  2*      0.5     /
'OBS'   'LGR2'  1       71      10      10      'OPEN'  2*      0.5     /
'OBS'   'LGR2'  1       72      10      10      'OPEN'  2*      0.5     /
'OBS'   'LGR2'  1       73      10      10      'OPEN'  2*      0.5     /
'OBS'   'LGR2'  1       74      10      10      'OPEN'  2*      0.5     /
'OBS'   'LGR2'  1       75      10      10      'OPEN'  2*      0.5     /
'OBS'   'LGR2'  1       76      10      10      'OPEN'  2*      0.5     /
'OBS'   'LGR2'  1       77      10      10      'OPEN'  2*      0.5     /
'OBS'   'LGR2'  1       78      10      10      'OPEN'  2*      0.5     /
'OBS'   'LGR2'  1       79      10      10      'OPEN'  2*      0.5     /
'OBS'   'LGR2'  1       80      10      10      'OPEN'  2*      0.5     /
'OBS'   'LGR2'  1       81      10      10      'OPEN'  2*      0.5     /
'OBS'   'LGR2'  1       82      10      10      'OPEN'  2*      0.5     /
'OBS'   'LGR2'  1       83      10      10      'OPEN'  2*      0.5     /
'OBS'   'LGR2'  1       84      10      10      'OPEN'  2*      0.5     /
'OBS'   'LGR2'  1       85      10      10      'OPEN'  2*      0.5     /
'OBS'   'LGR2'  1       86      10      10      'OPEN'  2*      0.5     /
'OBS'   'LGR2'  1       87      10      10      'OPEN'  2*      0.5     /
'OBS'   'LGR2'  1       88      10      10      'OPEN'  2*      0.5     /
'OBS'   'LGR2'  1       89      10      10      'OPEN'  2*      0.5     /
'OBS'   'LGR2'  1       90      10      10      'OPEN'  2*      0.5     /
'OBS'   'LGR2'  1       91      10      10      'OPEN'  2*      0.5     /
'OBS'   'LGR2'  1       92      10      10      'OPEN'  2*      0.5     /
'OBS'   'LGR2'  1       93      10      10      'OPEN'  2*      0.5     /
'OBS'   'LGR2'  1       94      10      10      'OPEN'  2*      0.5     /
'OBS'   'LGR2'  1       95      10      10      'OPEN'  2*      0.5     /
'OBS'   'LGR2'  1       96      10      10      'OPEN'  2*      0.5     /
'OBS'   'LGR2'  1       97      10      10      'OPEN'  2*      0.5     /
'OBS'   'LGR2'  1       98      10      10      'OPEN'  2*      0.5     /
'OBS'   'LGR2'  1       99      10      10      'OPEN'  2*      0.5     /
'OBS'   'LGR2'  1       100     10      10      'OPEN'  2*      0.5     /
/

WFRICTNL
'INJ' 0.5 0.0005 /
'LGR1'  5       1       10      0       10      /
'LGR1'  5       2       10      10      20      /
'LGR1'  5       3       10      20      30      /
'LGR1'  5       4       10      30      40      /
'LGR1'  5       5       10      40      50      /
'LGR1'  5       6       10      50      60      /
'LGR1'  5       7       10      60      70      /
'LGR1'  5       8       10      70      80      /
'LGR1'  5       9       10      80      90      /
'LGR1'  5       10      10      90      100     /
'LGR1'  5       11      10      100     110     /
'LGR1'  5       12      10      110     120     /
'LGR1'  5       13      10      120     130     /
'LGR1'  5       14      10      130     140     /
```

```
'LGR1'  5   15   10   140   150   /
'LGR1'  5   16   10   150   160   /
'LGR1'  5   17   10   160   170   /
'LGR1'  5   18   10   170   180   /
'LGR1'  5   19   10   180   190   /
'LGR1'  5   20   10   190   200   /
'LGR1'  5   21   10   200   210   /
'LGR1'  5   22   10   210   220   /
'LGR1'  5   23   10   220   230   /
'LGR1'  5   24   10   230   240   /
'LGR1'  5   25   10   240   250   /
'LGR1'  5   26   10   250   260   /
'LGR1'  5   27   10   260   270   /
'LGR1'  5   28   10   270   280   /
'LGR1'  5   29   10   280   290   /
'LGR1'  5   30   10   290   300   /
'LGR1'  5   31   10   300   310   /
'LGR1'  5   32   10   310   320   /
'LGR1'  5   33   10   320   330   /
'LGR1'  5   34   10   330   340   /
'LGR1'  5   35   10   340   350   /
'LGR1'  5   36   10   350   360   /
'LGR1'  5   37   10   360   370   /
'LGR1'  5   38   10   370   380   /
'LGR1'  5   39   10   380   390   /
'LGR1'  5   40   10   390   400   /
'LGR1'  5   41   10   400   410   /
'LGR1'  5   42   10   410   420   /
'LGR1'  5   43   10   420   430   /
'LGR1'  5   44   10   430   440   /
'LGR1'  5   45   10   440   450   /
'LGR1'  5   46   10   450   460   /
'LGR1'  5   47   10   460   470   /
'LGR1'  5   48   10   470   480   /
'LGR1'  5   49   10   480   490   /
'LGR1'  5   50   10   490   500   /
'LGR1'  5   51   10   500   510   /
'LGR1'  5   52   10   510   520   /
'LGR1'  5   53   10   520   530   /
'LGR1'  5   54   10   530   540   /
'LGR1'  5   55   10   540   550   /
'LGR1'  5   56   10   550   560   /
'LGR1'  5   57   10   560   570   /
'LGR1'  5   58   10   570   580   /
'LGR1'  5   59   10   580   590   /
'LGR1'  5   60   10   590   600   /
'LGR1'  5   61   10   600   610   /
'LGR1'  5   62   10   610   620   /
'LGR1'  5   63   10   620   630   /
'LGR1'  5   64   10   630   640   /
'LGR1'  5   65   10   640   650   /
```

```
'LGR1'  5       66      10      650     660     /
'LGR1'  5       67      10      660     670     /
'LGR1'  5       68      10      670     680     /
'LGR1'  5       69      10      680     690     /
'LGR1'  5       70      10      690     700     /
'LGR1'  5       71      10      700     710     /
'LGR1'  5       72      10      710     720     /
'LGR1'  5       73      10      720     730     /
'LGR1'  5       74      10      730     740     /
'LGR1'  5       75      10      740     750     /
'LGR1'  5       76      10      750     760     /
'LGR1'  5       77      10      760     770     /
'LGR1'  5       78      10      770     780     /
'LGR1'  5       79      10      780     790     /
'LGR1'  5       80      10      790     800     /
'LGR1'  5       81      10      800     810     /
'LGR1'  5       82      10      810     820     /
'LGR1'  5       83      10      820     830     /
'LGR1'  5       84      10      830     840     /
'LGR1'  5       85      10      840     850     /
'LGR1'  5       86      10      850     860     /
'LGR1'  5       87      10      860     870     /
'LGR1'  5       88      10      870     880     /
'LGR1'  5       89      10      880     890     /
'LGR1'  5       90      10      890     900     /
'LGR1'  5       91      10      900     910     /
'LGR1'  5       92      10      910     920     /
'LGR1'  5       93      10      920     930     /
'LGR1'  5       94      10      930     940     /
'LGR1'  5       95      10      940     950     /
'LGR1'  5       96      10      950     960     /
'LGR1'  5       97      10      960     970     /
'LGR1'  5       98      10      970     980     /
'LGR1'  5       99      10      980     990     /
'LGR1'  5       100     10      990     1000    /
/
WFRICTNL
'OBS' 0.5 0.0005 /
'LGR2'  1       1       10      0       10      /
'LGR2'  1       2       10      10      20      /
'LGR2'  1       3       10      20      30      /
'LGR2'  1       4       10      30      40      /
'LGR2'  1       5       10      40      50      /
'LGR2'  1       6       10      50      60      /
'LGR2'  1       7       10      60      70      /
'LGR2'  1       8       10      70      80      /
'LGR2'  1       9       10      80      90      /
'LGR2'  1       10      10      90      100     /
'LGR2'  1       11      10      100     110     /
'LGR2'  1       12      10      110     120     /
'LGR2'  1       13      10      120     130     /
```

```
'LGR2'  1       14      10      130     140     /
'LGR2'  1       15      10      140     150     /
'LGR2'  1       16      10      150     160     /
'LGR2'  1       17      10      160     170     /
'LGR2'  1       18      10      170     180     /
'LGR2'  1       19      10      180     190     /
'LGR2'  1       20      10      190     200     /
'LGR2'  1       21      10      200     210     /
'LGR2'  1       22      10      210     220     /
'LGR2'  1       23      10      220     230     /
'LGR2'  1       24      10      230     240     /
'LGR2'  1       25      10      240     250     /
'LGR2'  1       26      10      250     260     /
'LGR2'  1       27      10      260     270     /
'LGR2'  1       28      10      270     280     /
'LGR2'  1       29      10      280     290     /
'LGR2'  1       30      10      290     300     /
'LGR2'  1       31      10      300     310     /
'LGR2'  1       32      10      310     320     /
'LGR2'  1       33      10      320     330     /
'LGR2'  1       34      10      330     340     /
'LGR2'  1       35      10      340     350     /
'LGR2'  1       36      10      350     360     /
'LGR2'  1       37      10      360     370     /
'LGR2'  1       38      10      370     380     /
'LGR2'  1       39      10      380     390     /
'LGR2'  1       40      10      390     400     /
'LGR2'  1       41      10      400     410     /
'LGR2'  1       42      10      410     420     /
'LGR2'  1       43      10      420     430     /
'LGR2'  1       44      10      430     440     /
'LGR2'  1       45      10      440     450     /
'LGR2'  1       46      10      450     460     /
'LGR2'  1       47      10      460     470     /
'LGR2'  1       48      10      470     480     /
'LGR2'  1       49      10      480     490     /
'LGR2'  1       50      10      490     500     /
'LGR2'  1       51      10      500     510     /
'LGR2'  1       52      10      510     520     /
'LGR2'  1       53      10      520     530     /
'LGR2'  1       54      10      530     540     /
'LGR2'  1       55      10      540     550     /
'LGR2'  1       56      10      550     560     /
'LGR2'  1       57      10      560     570     /
'LGR2'  1       58      10      570     580     /
'LGR2'  1       59      10      580     590     /
'LGR2'  1       60      10      590     600     /
'LGR2'  1       61      10      600     610     /
'LGR2'  1       62      10      610     620     /
'LGR2'  1       63      10      620     630     /
'LGR2'  1       64      10      630     640     /
```

```
'LGR2'  1       65      10      640     650     /
'LGR2'  1       66      10      650     660     /
'LGR2'  1       67      10      660     670     /
'LGR2'  1       68      10      670     680     /
'LGR2'  1       69      10      680     690     /
'LGR2'  1       70      10      690     700     /
'LGR2'  1       71      10      700     710     /
'LGR2'  1       72      10      710     720     /
'LGR2'  1       73      10      720     730     /
'LGR2'  1       74      10      730     740     /
'LGR2'  1       75      10      740     750     /
'LGR2'  1       76      10      750     760     /
'LGR2'  1       77      10      760     770     /
'LGR2'  1       78      10      770     780     /
'LGR2'  1       79      10      780     790     /
'LGR2'  1       80      10      790     800     /
'LGR2'  1       81      10      800     810     /
'LGR2'  1       82      10      810     820     /
'LGR2'  1       83      10      820     830     /
'LGR2'  1       84      10      830     840     /
'LGR2'  1       85      10      840     850     /
'LGR2'  1       86      10      850     860     /
'LGR2'  1       87      10      860     870     /
'LGR2'  1       88      10      870     880     /
'LGR2'  1       89      10      880     890     /
'LGR2'  1       90      10      890     900     /
'LGR2'  1       91      10      900     910     /
'LGR2'  1       92      10      910     920     /
'LGR2'  1       93      10      920     930     /
'LGR2'  1       94      10      930     940     /
'LGR2'  1       95      10      940     950     /
'LGR2'  1       96      10      950     960     /
'LGR2'  1       97      10      960     970     /
'LGR2'  1       98      10      970     980     /
'LGR2'  1       99      10      980     990     /
'LGR2'  1       100     10      990     1000    /
/

WPIMULT
'INJ' 0.5 5*/
'OBS' 0.5 5*/
/

WCONINJ
'INJ' 'WATER' 'OPEN' 'RATE' 500 /
/

WCONPROD
'OBS'   'OPEN'   'RATE'   4*  0 /
/
```

```
TSTEP
--IMPLEMET INCREASING LOGARITMIC TIME
0.00006  8.20267E-05  0.00011214  0.000153308  0.000209589  0.000286531  0.000391721
0.000535526     0.000732124     0.001000896     0.001368337     0.00187067     0.002557416
0.003496275
0.004779801     0.006534524     0.008933428     0.012213     0.016696542     0.022826047
0.031205769
0.042661789     0.058323456     0.079734712     0.109006303     0.149023855     0.203732341
0.278524984
0.380774923     0.52056207      0.711666794     0.972928408     1.330102366     1.818399267
2.485955953
3.398580891  4.646241642  6.351933967  8.683806876  11.87173895  16.23
/

WCONINJ
'INJ' 'WATER' 'STOP' 'RATE' 500 3*/
/
WCONPROD
'OBS'   'OPEN'   'RATE'   4*  0 /
/

TSTEP
0.00006  8.20267E-05  0.00011214  0.000153308  0.000209589  0.000286531  0.000391721
0.000535526     0.000732124     0.001000896     0.001368337     0.00187067     0.002557416
0.003496275
0.004779801     0.006534524     0.008933428     0.012213     0.016696542     0.022826047
0.031205769
0.042661789     0.058323456     0.079734712     0.109006303     0.149023855     0.203732341
0.278524984
0.380774923     0.52056207      0.711666794     0.972928408     1.330102366     1.818399267
2.485955953
3.398580891  4.646241642  6.351933967  8.683806876  11.87173895  16.23
/

END
```